Check for updates

Received: 1 December 2021 | Revised: 22 May 2022 | Accepted: 23 May 2022

DOI: 10.1111/apha.13845

ACTA PHYSIOLOGICA

RESEARCH PAPER

Dining on the dead in the deep: Active NH_4^+ excretion via $Na^+/H^+(NH_4^+)$ exchange in the highly ammonia tolerant Pacific hagfish, *Eptatretus stoutii*

Alexander M. Clifford[1,2,3] | **Michael P. Wilkie**[4] | **Susan L. Edwards**[5] | **Martin Tresguerres**[1] | **Greg G. Goss**[2,3]

[1]Marine Biology Research Division, Scripps Institution of Oceanography, University of California, La Jolla, California, USA

[2]Department of Biological Sciences, University of Alberta, Edmonton, Alberta, Canada

[3]Bamfield Marine Sciences Centre, Bamfield, British Columbia, Canada

[4]Department of Biology and Laurier Institute for Water Science, Wilfrid Laurier University, Waterloo, Ontario, Canada

[5]Department of Biological Sciences, Wright State University, Dayton, Ohio, USA

Correspondence
Alexander M. Clifford, University of California San Diego Scripps Institution of Oceanography, Marine Biology Research Division, 8750 Biological Grade, La Jolla, CA 92093-5004, USA.
Email: alex.clifford@me.com

Funding information
National Science Foundation, Grant/Award Number: 1121369 and 1754994; Natural Sciences and Engineering Research Council of Canada, Grant/Award Number: 04248 and 702306

Abstract

Aim: Pacific hagfish are exceptionally tolerant to high environmental ammonia (HEA). Here, we elucidated a cellular mechanism that enables hagfish to actively excrete ammonia against steep ammonia gradients expected to be found inside a decomposing whale carcass.

Methods: Hagfish were exposed to varying concentrations of HEA in the presence or absence of environmental Na^+, while plasma ammonia levels were tracked. ^{14}C-methylammonium was used as a proxy for NH_4^+ to measure efflux in whole animals and in isolated gill pouches; the latter allowed us to assess the effects of amiloride specifically on Na^+/H^+ exchangers (NHEs) in gill cells. Western blotting and immunohistochemistry were utilized to evaluate the abundance and subcellular localization of Rhesus glycoprotein (Rh) channels in the response to HEA.

Results: Hagfish actively excreted NH_4^+ against steep inwardly directed E_{NH4}^+ ($\Delta E_{NH4}^+ \sim 35$ mV) and pNH_3 ($\Delta pNH_3 \sim 2000$ µtorr) gradients. Active NH_4^+ excretion and plasma ammonia hypo-regulation were contingent on the presence of environmental Na^+, indicating a Na^+/NH_4^+ exchange mechanism. Active NH_4^+ excretion across isolated gill pouches was amiloride-sensitive. Exposure to HEA resulted in decreased abundance of Rh channels in the apical membrane of gill ionocytes.

Conclusions: During HEA exposure, hagfish can actively excrete ammonia against a steep concentration gradient using apical NHEs energized by Na^+-K^+-ATPase in gill ionocytes. Additionally, apical Rh channels are removed from the apical membrane, presumably to reduce ammonia loading from the environment. We suggest that this mechanism allows hagfish to maintain tolerable ammonia levels while feeding inside decomposing carrion, allowing them to exploit nutrient-rich food-falls.

KEYWORDS

Agnatha, ammonium, gill, high environmental ammonia, Na^+/H^+ exchanger, Na^+/NH_4^+ exchange, nitrogen, rhesus glycoprotein

Martin Tresguerres and Greg G. Goss contributed equally to this work.

© 2022 Scandinavian Physiological Society. Published by John Wiley & Sons Ltd.

1 | INTRODUCTION

The carcasses of whales laying on the ocean floor yield an abundance of nutrients for benthic necrophages, and are biodiversity oases that can sustain up to 400 different species through the successional stages of decomposition.[1,2] Mobile necrophages arrive within hours after a whale carcass settles and will persist in the area for months to years until the soft tissues have been completely consumed. In the initial stages, necrophages include hagfish, rat-tail chimeras, sleeper sharks, crabs, and amphipods. Of these, hagfish are usually first on site and represent the largest biomass.[1,3] Indeed, hagfish are renowned for their critical role in benthic organic nutrient cycling of whalefalls and other benthic carrion.[3]

Scavenging inside a whale carcass entails significant physiological challenges, as the metabolism of necrophages and decomposing bacteria consume O_2 and generate CO_2 and ammonia.[4] Accordingly, hagfish are exceptionally tolerant to hypoxia,[5] hypercapnia,[6,7] and high environmental ammonia (HEA).[8,9] Hagfish hypoxia tolerance is achieved by a low metabolic rate, efficient O_2 uptake at the gill, and high anaerobic capacity of tissues, including the myocardium.[10–13]

Hagfishes can survive large swings in blood pH (±1 pH unit) from both metabolic and respiratory acid–base disturbances. Their hypercapnia tolerance is the result of being able to excrete massive amounts of H^+ across their gills, and an unmatched ability to accumulate large amounts of plasma HCO_3^- in order to offset respiratory acidosis.[6,7,14–17] HCO_3^- loading and unloading occurs equimolarly in exchange for plasma Cl^-,[6,7] and the capacity for hagfish to regulate plasma [HCO_3^-] to extraordinary levels (>80 mM) may be linked to their osmo-conforming strategy. Overall, this strategy would therefore yield a greater plasma Cl^- pool (~400–500 mM Cl^-) for branchial anion exchange compared to other aquatic vertebrates (100–150 mM Cl^-).[18,19]

Hagfishes' tolerance to HEA is equally fascinating: while most other water-breathing fishes experience acutely lethal ammonia toxicity during exposure to just 0.5–1 mM ammonia,[20] hagfish can survive an exposure to 20 mM ammonia for 48 h or more. During this time, they hypo-regulate their plasma ammonia levels at ~5 mM, roughly four-fold less than in the environment.[9] Furthermore, previous studies have reported that hagfish can survive exposure to HEA as high as 100 mM.[8] These abilities yield significant competitive advantages over other necrophages and opportunistic feeders and are therefore likely essential to the evolutionary success of hagfish. However, the underlying mechanisms affording them exceptional ammonia tolerance are unresolved.

Animals constantly produce ammonia as a waste product of protein catabolism and other routine metabolic processes; because of its very high toxicity, ammonia must therefore be excreted or converted to other nitrogenous waste produces such as urea, glutamine, or uric acid.[20] Under control conditions, this metabolism generates outwardly directed gradients that favor the excretion of NH_3 gas and ionic NH_4^+. In vertebrates, NH_3 diffusive excretion is facilitated by Rhesus glycoprotein channels (Rh channels; Slc42a2-Slc42a3) on the apical (Rhcg) and basolateral (Rhbg) membranes of epithelial cells.[21–24] In renal tubules of mammals and in gills and skin of freshwater fishes, apical Rhcg can be functionally coupled to H^+-excreting Na^+ /H^+ exchangers (NHE; slc9a1-slc9a9) or V-type H^+-ATPase (VHA). This H^+ excretion results in the acid trapping of NH_3 as NH_4^+ in the external medium and thereby maintains an outwardly directed NH_3 diffusive gradient, thus enhancing NH_3 excretion.[22,24,25]

Hagfish have Rh channels in their gill and skin epithelia,[23,26] and upon ammonia loading induced by NH_4Cl infusion, they exhibit a rapid increase in gill Rhcg protein abundance,[23] consistent with their role in facilitating ammonia excretion across the apical membrane. However, for hagfish, a more ecologically relevant scenario of continuous exposure to HEA presents a different physiological challenge compared to direct infusion because it entails persistent inwardly directed NH_4^+ electrochemical and NH_3 partial pressure gradients. Thus, the presence of apical Rh channels would enhance ammonia influx and subsequent accumulation in plasma and tissues. However, during HEA exposure, Pacific hagfish can hypo-regulate plasma total ammonia concentrations ($[T_{amm}]_p$) well below ambient concentrations.[9] Notably, hypo-regulation is not associated with conversion of ammonia to alternative end-products such as glutamine or urea,[9] a strategy observed in air-breathing ammonia tolerant fishes.[27,28] Furthermore, hagfish metabolic rate is unabated during HEA exposure,[29] thus adding metabolically produced ammonia to exogenous ammonia loading. Taken together, these observations indicate that the ability of hagfish to hypo-regulate $[T_{amm}]_p$ during HEA exposure is achieved by active NH_4^+ excretion through a yet unidentified mechanism, possibly coupled to reduced permeability to environmental NH_3 to minimize loading.

While Krogh (1938) originally postulated that NH_4^+ could be exchanged for Na^+ in the gills of freshwater goldfish,[30] this mechanism has only been conclusively demonstrated in the medullary thick ascending loop of Henle of the mammalian kidney.[24,31] Furthermore, recent crystal structure analysis of NHE binding sites indicate that H^+ are actually transported as H_3O^+ which is similar to NH_4^+ in both molecular mass (19.02 a.u. vs 18.04 a.u., respectively) and ionic radius (100 Å vs 133 Å, respectively).[32] In aquatic vertebrates, active ammonia excretion via apical

NHE (and powered by basolateral NKA) was first proposed to operate in the gills of the air-breathing mudskipper (*Periophthalmodon schlosseri*) ~25 years ago based on amiloride sensitivity of ammonia excretion in 50% seawater[33]; however, to our knowledge, no functional studies have yet convincingly demonstrated Na^+/NH_4^+ exchange by NHE in any organism.

Here, we hypothesized that an active mechanism mediates active NH_4^+ excretion across hagfish gills during exposure to HEA. Importantly, hagfish gill ion-transporting cells ("ionocytes") abundantly express NHEs and Na^+/K^+-ATPase (NKA).[14,34,35] Since NKA activity lowers intracellular Na^+ concentration well below that of seawater, it would allow for a persistent inwardly directed Na^+ gradient sufficient to drive NH_4^+ excretion through apical NHEs during HEA.

To test our hypotheses, we first performed an in vitro experiment to explore the levels of HEA that could theoretically be encountered by hagfish inside a decomposing carcass. Next, we confirmed hagfish can actively excrete ammonia during HEA exposure through flux measurements of ^{14}C-methylamine (^{14}C-MA) as a proxy for NH_4^+ flux (J_{NH4+}). We then evaluated whether environmental Na^+ acts as a counterion for NH_4^+ excretion by measuring J_{NH4+} and $[T_{amm}]_p$ levels during HEA exposure in Na^+-free seawater. To specifically assess the role of the gill over other potential ammonia excretory organs such as the skin and the kidneys, we developed a novel in situ gill pouch double perfusion/perifusion technique to measure J_{NH4+} and evaluate its sensitivity to the NHE inhibitor amiloride. Finally, we evaluated the roles of Rh channels in modulating NH_3 permeability by examining their abundance and sub-cellular localization in gills from control and HEA exposed hagfish. We conclude that hagfish use apical NHEs to actively excrete NH_4^+ during exposure to HEA, and that removal of Rh channels from the apical membrane of gill ionocytes acts to prevent NH_3 accumulation/back-flux during HEA exposure. This mechanism allows the scavenging hagfish to exploit the nutrient-rich, but noxious interiors of putrefying marine fishes and marine mammals.

2 | RESULTS

2.1 | Experiment 1: Controlled rotting of animal tissue in seawater

Bovine (*Bos taurus*) muscle and liver tissues were left to incubate within sealed chambers containing seawater for up to 17 days alongside tissue-free control chambers. Within 24 h, $[T_{amm}]_w$ reached ~7 mM in muscle-containing chambers and ~19 mM in liver-containing chambers. In tissue-containing chambers, $[T_{amm}]_w$ continued to rise significantly in a time-dependent manner (Figure 1A; muscle: $[T_{amm}]_w = 5.4\,mM\,day^{-1}$ x time (days); liver: $[T_{amm}]_w = 5.0\,mM\,day^{-1}$ x time (days)) reaching ~85–95 mM by day 17 in tissue-containing chambers. The slopes of these trends were significantly different ($F_{2,66} = 44.47$, $p < 0.0001$) compared to $[T_{amm}]_w$ trends in the tissue-free control chambers ($[T_{amm}]_w = 1.3\,\mu M\,day^{-1}$ x time (days)) where $[T_{amm}]_w$ remained low (<30 μM) throughout the course of the experiment.

Water pH (pH_w) and TCO_2 (total CO_2) measurements during decomposition were used to calculate pCO_2 (Figure 1B). Two-way repeated measures ANOVA with Giesser-Greenhouse correction revealed significant main effects of tissue type, time, and the interaction between tissue and time on pH (tissue type: $F_{2,6} = 439.6$, $p < 0.0001$; time: $F_{2.877,17.26} = 156.3$, $p < 0.0001$; interaction: $F_{14,42} = 41.69$, $p < 0.0001$) and pCO_2 (tissue type: $F_{2,6} = 477$, $p < 0.0001$; time: $F_{1.110,6.659} = 390.4$, $p < 0.0001$; interaction: $F_{14,42} = 94.17$, $p < 0.0001$). Both water pH and pCO_2 in tissue-free control chambers remained virtually unchanged in the initial 4 days of the incubations, and only showed mild acidification by day 12 and 17. In contrast, the pH_w in chambers containing bovine tissues significantly decreased after just 12 h from initial pH values of ~7.9 down to pH 6.0–6.2 (muscle: $p = 0.0036$; liver: $p = 0.074$). The pH_w continued to decrease throughout the incubations, reaching pH 5.4–6.0 in muscle-containing chambers ($p \leq 0.0088$), and even lower pH 4.3–5.4 in liver-containing chambers ($p \leq 0.0114$).

Similarly, water pCO_2 in tissue-containing chambers increased ~30-fold within 12 h, reaching ~15–20 torr. From days 1–12, water pCO_2 continued to rise and ranged from 25–35 torr CO_2. Most notably, water pCO_2 reached values as high as 300 torr in both muscle-containing and liver-containing chambers on day 17 ($p < 0.0001$).

2.2 | Experiment 2: $[T_{amm}]_p$ regulation during HEA exposure

Hagfish plasma total ammonia concentration ($[T_{amm}]_p$) was tracked during continued exposure to HEA of varying magnitude. Ordinary two-way ANOVA revealed significant main effects of time ($F_{3,120} = 10.78$, $p < 0.0001$), $[T_{amm}]_w$ ($F_{5,120} = 219.1$, $p < 0.0001$), and the interaction between time and $[T_{amm}]_w$ ($F_{15,120} = 3.283$, $p < 0.0001$). In control hagfish exposed to nominally ammonia-free conditions, $[T_{amm}]_p$ averaged ~100 μM and did not deviate significantly throughout the experiment, while exposure to increasing levels of environmental ammonia resulted in dose- and time-dependent increases in $[T_{amm}]_p$ (Figure 2A). Compared to control hagfish, $[T_{amm}]_p$ was significantly greater in hagfish exposed to 1-,

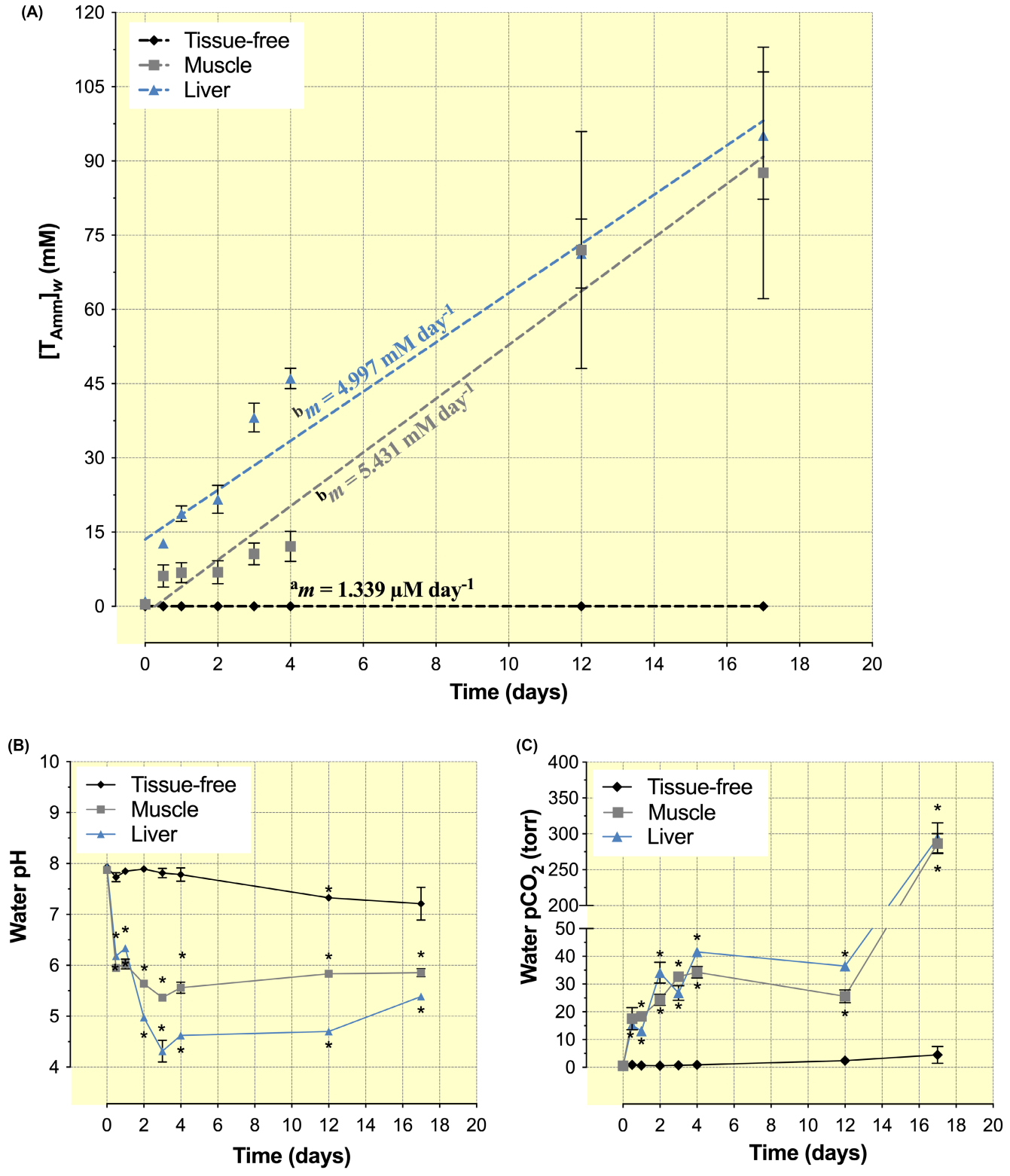


FIGURE 1 Determination of ammonia generation, acid–base, and pCO_2 dynamics during marine decomposition. Tissue samples (~1 g) of either bovine (*Bos taurus*) muscle (gray squares) or liver (blue triangles) tissues were incubated at 12°C within sealed syringes containing unfiltered seawater, with water samples removed periodically over a 17-day period and analyzed for (A) $[T_{amm}]_w$, (B) water pH, and (C) water pCO_2. Data are presented as mean ± s.e.m. In (A), Slope (m) values for best-fit lines (dashed lines) are displayed in bold lettering, while significant differences amongst slopes are denoted by slope values not sharing superscripted letters ($p < 0.0001$; linear regression analysis with comparison of slopes). Values of (b) pH_w, and (c) Water pCO_2 significantly different from t = 0 values are denoted by an asterisk (*) ($p < 0.05$; Two-way repeated measures ANOVA with Geisser–Greenhouse correction and Dunnett's *post-hoc* analysis). $n = 3$.

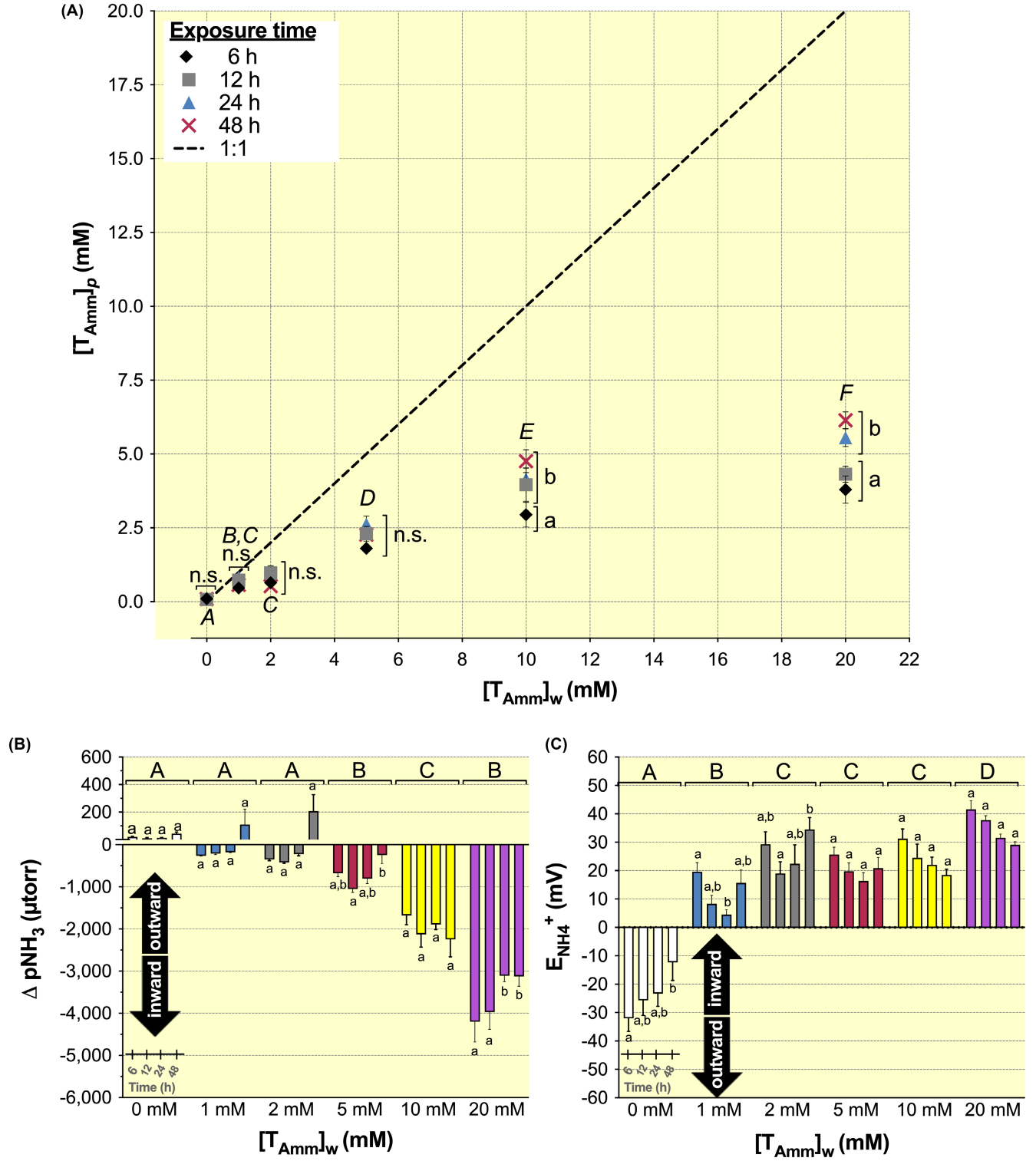


FIGURE 2 Stabilization of $[T_{amm}]_p$ below environmental levels during 48 h HEA exposure over a range of nominal HEA concentrations. (A) $[T_{amm}]_p$ stabilized below line of equivalence (hashed line) at approximately ~2.5:1 plasma: water $[T_{amm}]$, despite sustained elevation in (B) ΔpNH_3 (partial pressure of NH_3) and (C) E_{NH4}^+ (Nernst equilibrium potential for NH_4^+) gradients. In (b) note the different scales on the positive and negative y-axis. In (B) and (C), data are presented sequentially over time within each exposure group (i.e., bars represent 6, 12, 24, 48 h from left to right), positive ΔpNH_3 values denote outwardly directed blood-to-water pNH_3 gradients and negative E_{NH4}^+ values denote outwardly directed NH_4^+ gradients. Main inter-group differences are denoted by exposure groups not sharing upper-case letters while intra-group differences over exposure time are denoted by data-points not sharing lower-case letters ($p < 0.05$; Ordinary two-way ANOVA with Tukey's *post-hoc* analysis). $n = 6$.

2-, and 5-mM HEA ($p \leq 0.0424$; mean of samples across all time-points = 0.65, 0.78 and 2.25 mM, respectively); however, no differences in $[T_{amm}]_p$ were observed throughout the time-course within these three exposure groups ($p > 0.136$). In contrast, $[T_{amm}]_p$ was significantly elevated in animals exposed to 10- and 20-mM HEA (mean = 3.96 and 4.95 mM over all time points respectively) compared to control hagfish ($p < 0.0001$), and at these higher HEA concentrations temporally dependent increases in $[T_{amm}]_p$ were observed whereby $[T_{amm}]_p$ stabilized only after 12 h in the 10 mM treatment and 24 h in the 20 mM treatment.

Stabilization of $[T_{amm}]_p$ occurred despite the continued presence of large inwardly directed driving gradients for NH_3 and NH_4^+ (Figure 2B,C). Ordinary two-way ANOVA on ΔpNH_3 and E_{NH4}^+ data revealed significant main effects of time, $[T_{amm}]_w$ and the interaction between time and $[T_{amm}]_w$ each of these calculated metrics (ΔpNH_3: [time: $F_{3,120} = 5.376$, $p = 0.0017$; $[T_{amm}]_w$: $F_{5,120} = 217.7$, $p < 0.0001$; interaction: $F_{15,120} = 2.158$, $p = 0.0114$]; E_{NH4}^+: [time: $F_{3,120} = 4.321$, $p = 0.0062$; $[T_{amm}]_w$: $F_{5,120} = 116.3$, $p < 0.0001$; interaction: $F_{15,120} = 2.423$, $p = 0.0041$]). Under control conditions, partial pressure and driving gradients for both NH_3 and NH_4^+ were outwardly directed (ΔpNH_3 = 10–43 μtorr, $E_{NH4}^+ = -12$ to -32 mV throughout 48 h of exposure). However, during HEA exposure the gradients for NH_3 and NH_4^+ reversed and increased inwardly in a dose-dependent manner.

Over the course of this experiment, water pH (Table 1) remained relatively constant throughout exposure (two-way repeated measures ANOVA with Geisser–Greenhouse correction; time: $F_{1.115,6.688} = 2.193$, $p = 0.1853$; concentration: $F_{5,6} = 1.538$, P = 3.057; interaction: $F_{5,18} = 0.8880$, $p = 0.5874$), while effects due to time ($F_{3,120} = 10.81$; $p < 0.0001$) concentration ($F_{5,120} = 11.93$; $p < 0.0001$) and the interaction between the two metrics ($F_{15,120} = 3.060$; $p = 0.0003$) were observed (Table 2). In general, compared to control (0 mM HEA) exposed animals, there was an alkalinizing effect of HEA exposure on blood pH within the first 6–12 h of exposure, and by 24–48 h, blood pH returned to levels no different to control levels.

2.3 | Experiment 3: Role for environmental Na^+ in the stabilization of $[T_{amm}]_p$ during HEA exposure

To determine the role of environmental Na^+ on $[T_{amm}]_p$ hypo-regulation during HEA exposure, hagfish were first acclimated to 10 mM HEA for 24 h to induce $[T_{amm}]_p$ accumulation to ≥2 mM. Hagfish were then transferred into 10 mM HEA in either Na^+-containing or Na^+-free artificial seawater (HEA/Na^+ and HEA/Na^+-Free, respectively) and $[T_{amm}]_p$ was tracked for 5 h post-transfer (Figure 3). Two-way repeated measures ANOVA with Geisser–Greenhouse correction revealed significant main effects of time ($F_{1.281,15.37} = 8.510$, $p = 0.0071$), presence of Na^+

TABLE 1 Time-course of water pH over 48 h at indicated $[T_{amm}]_w$ during Experiment 2

	$[T_{amm}]_w$ (μM)					
Time (h)	**0**	**1000**	**2000**	**5000**	**10 000**	**20 000**
6	8.16 ± 0.06	8.14 ± 0.02	7.98 ± 0.02	7.96 ± 0.02	8.04 ± 0.04	7.95 ± 0.06
12	8.15 ± 0.05	8.13 ± 0.02	8.04 ± 0.06	8.08 ± 0.00	8.08 ± 0.01	7.96 ± 0.08
24	8.11 ± 0.03	8.14 ± 0.02	7.86 ± 0.25	8.02 ± 0.06	8.04 ± 0.03	7.94 ± 0.02
48	8.14 ± 0.03	8.08 ± 0.01	7.58 ± 0.45	7.69 ± 0.31	8.10 ± 0.04	7.96 ± 0.00

Note: No overall differences were observed ($p > 0.05$; Two-way repeated measures ANOVA with Geisser–Greenhouse correction). $n = 2$.

TABLE 2 Time-course of blood pH over 48 h at indicated $[T_{amm}]_w$ during Experiment 2

	$[T_{amm}]_w$ (μM)					
Time (h)	**0**	**1000**	**2000**	**5000**	**10 000**	**20 000**
6	$^{A}8.00 \pm 0.03^{a}$	$^{A}8.08 \pm 0.06^{a}$	$^{A}8.11 \pm 0.02^{a}$	$^{A}8.14 \pm 0.02^{a}$	$^{B}8.29 \pm 0.03^{a}$	$^{A}8.08 \pm 0.09^{a}$
12	$^{A}7.93 \pm 0.01^{a}$	$^{A,B}7.97 \pm 0.04^{a}$	$^{A,B}7.96 \pm 0.03^{a}$	$^{A,B}8.08 \pm 0.05^{a}$	$^{A,B}8.12 \pm 0.05^{a,b}$	$^{B}8.15 \pm 0.02^{a}$
24	7.98 ± 0.03^{a}	7.98 ± 0.03^{a}	7.96 ± 0.04^{a}	8.01 ± 0.02^{a}	8.08 ± 0.03^{b}	8.14 ± 0.02^{a}
48	$^{A,B}8.02 \pm 0.07^{a}$	$^{A}7.92 \pm 0.05^{a}$	$^{C}7.63 \pm 0.12^{b}$	$^{A,B}7.97 \pm 0.07^{a}$	$^{A,B}8.04 \pm 0.07^{b}$	$^{B,D}8.14 \pm 0.05^{a}$

Note: Data not sharing upper-case letters represent significant difference across concentrations at a given time-point, while data not sharing lower case letters within a treatment denotes significant differences over time ($p < 0.05$, Two-way ANOVA with Tukey's multiple comparison post hoc analysis). $n = 6$.

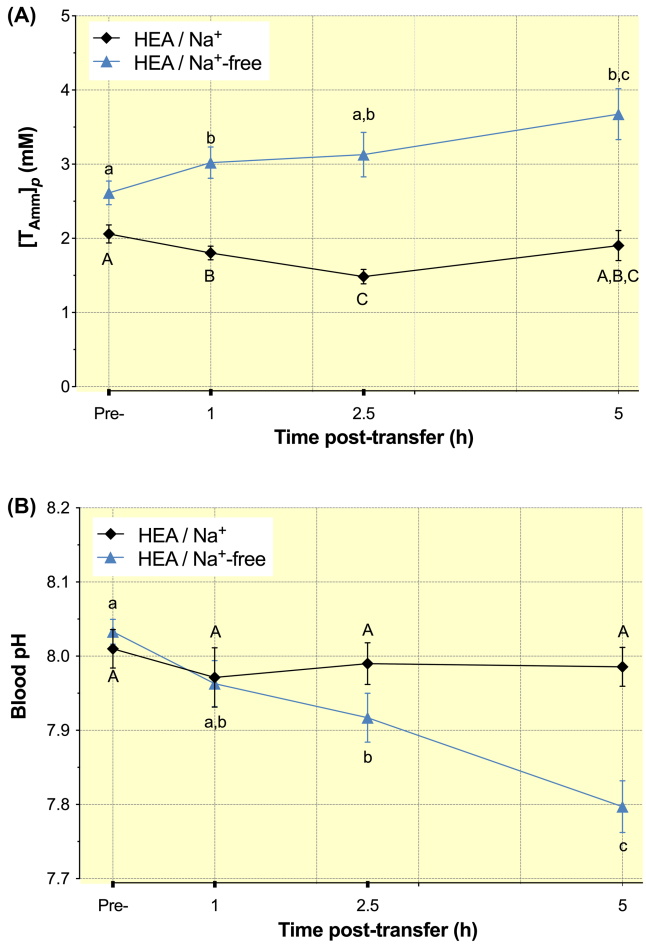


FIGURE 3 Hypo-regulation of plasma ammonia is dependent on environmental [Na^+]. (A) Plasma [T_{amm}] and (B) blood pH in hagfish pre-exposed to HEA (10 mmol/L) for 24 h, then transferred to Na^+-containing (HEA/Na^+) or Na^+-free artificial HEA seawater (HEA/Na^+-free). Data not sharing upper-case (HEA/Na^+), or lower-case (HEA/Na^+-free) letters denote significant differences ($p < 0.05$; Two-way repeated measures ANOVA with Geisser–Greenhouse correction and Tukey's *post-hoc* analysis). $n = 6$–7.

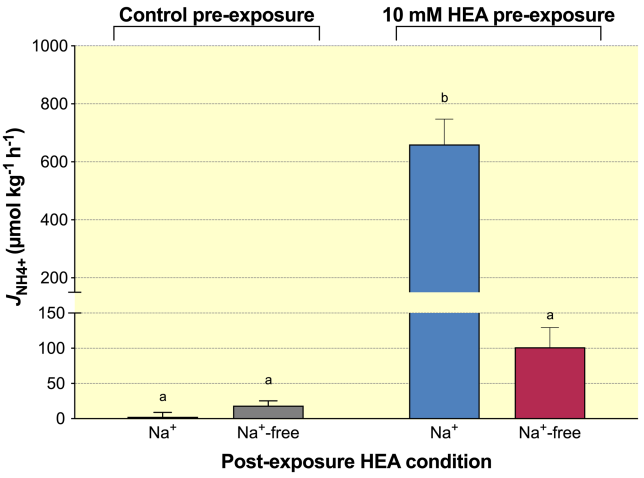


FIGURE 4 Active ammonia excretion is dependent on environmental [Na^+]. Hagfish were pre-exposed to either HEA (10 mmol/L) or non-HEA (control) conditions for 18 h, injected with a radiolabeled analog of NH_4^+ (^{14}C-methylammonium), then promptly returned to exposure conditions for an additional 6 h (24 h total pre-exposure). Following pre-exposure, hagfish were transferred into either Na^+-containing or Na^+-free artificial HEA sea water for 2.5 h. J_{NH4+} was calculated from appearance of ^{14}C-MA counts in flux media, measured blood pH, plasma T_{amm}, and ^{14}C-MA specific activity values on a per-animal basis. Bars not sharing letters denote significant differences ($p < 0.05$; Two-way ANOVA with Tukey's *post-hoc* analysis). $n = 6$.

($F_{1,12} = 23.72$, $p = 0.0004$) and the interaction between the two ($F_{3,36} = 12.89$, $p < 0.0001$) on [T_{amm}]$_p$. Following transfer to HEA/Na^+-containing water (control treatment), we observed a significant ~25% reduction in [T_{amm}]$_p$ within 2.5 h of transfer ($p = 0.0027$), which returned to levels that were not significantly different from pre-transfer concentrations by 5 h ($p = 0.1515$). However, transfer into HEA/Na^+-free (experimental treatment) induced a progressive increase in [T_{amm}]$_p$ that reached ~3.5 mM after 5 h of exposure: ~40% higher than pre-transfer [T_{amm}]$_p$; $p < 0.0001$).

Over the course of this experiment, we noted a significant effect of time ($F_{2.273,27.28} = 9.926$, $p = 0.0004$) and the interaction between time and treatment ($F_{3,36} = 7.595$; $p = 0.0005$) on blood pH (Figure 3B; Two-way repeated measures ANOVA with Geisser–Greenhouse correction). No significant differences were observed in the blood acid-base status following transfer to HEA/Na^+ conditions; however, animals transferred to HEA/Na^+-free conditions experienced a progressive acidosis from pH ~8.03 at 0 h post transfer to pH ~7.92 by 2.5 h ($p = 0.0459$) and pH ~7.80 by 5 h ($p = 0.0021$).

2.4 | Experiment 4: Determination of active and Na^+-dependent NH_4^+ excretion during HEA exposure

To determine the ability of hagfish to excrete NH_4^+ during HEA exposure, we measured the flux of ^{14}C-methylammonium as a proxy for NH_4^+ flux (J_{NH4+}). Hagfish were exposed to either control conditions or to 10 mM HEA for 18 h to induce ammonia accumulation. Hagfish were then injected with ^{14}C-methylammonium, and the isotope was allowed to equilibrate in the animal for another 6 h. At 24 h, hagfish were transferred to 10 mM HEA/Na^+ or HEA/Na^+-free conditions.

Ordinary two-way ANOVA revealed significant effects of exposure treatment (Figure 4; $F_{1,20} = 64.22$, $p < 0.0001$), presence of Na^+ ($F_{1,20} = 34.51$, $p < 0.0001$), and the interaction between exposure treatment and presence of Na^+ on J_{NH4+} ($F_{1,20} = 38.66$, $p < 0.0001$). In control-exposed hagfish, J_{NH4+} was low (<20 µmol kg^{-1} h^{-1}), regardless of

whether flux was measured in HEA/Na^+ or HEA/Na^+-free conditions ($p = 0.9948$). In contrast, hagfish that had been pre-exposed to 10 mM HEA exhibited significantly greater J_{NH4+} (660 ± 215 μmol kg^{-1} h^{-1}; $p < 0.0001$) in HEA/Na^+ conditions. Confirming the importance of environmental Na^+ for ammonia excretion, J_{NH4+} of hagfish exposed to HEA/Na^+-free conditions was significantly lower (101 ± 68 μmol kg^{-1} h^{-1}; $p < 0.0001$). Furthermore, this J_{NH4+} was not significantly different than that of hagfish from the control pre-exposure ($p = 0.4488$).

2.5 | Experiment 5: Effect of amiloride on NH_4^+ excretion across isolated gill pouches

J_{NH4+} was measured in gill pouches isolated from HEA exposed animals that were dually cannulated in situ to simulate blood flow and seawater current in gill pouches. This preparation allowed us to add ^{14}C-methylammonium in the plasma-like perfusate in the vascular side and measure its appearance in the perifusate after it had passed through the lumen of the gill pouch. (Figure 5A). Both the perfusate and the perifusate were spiked with ammonia to mimic the conditions measured previously in the whole-animal experiments (i.e., Figure 2A). Gill pouches perfused with hagfish saline +4 mM NH_4Cl + ^{14}C-methylammonium and perifused with 10 mM NH_4Cl on the external side demonstrated outwardly directed J_{NH4+} that averaged 457 ± 102 nmol g dry tissue^{-1} min^{-1} (Figure 5B). However, gill pouches perifused under the same conditions, but with 500 μM amiloride in the perifusate, had significantly lower J_{NH4+} (176 ± 54 nmol g dry tissue^{-1} min^{-1}, $p = 0.0069$).

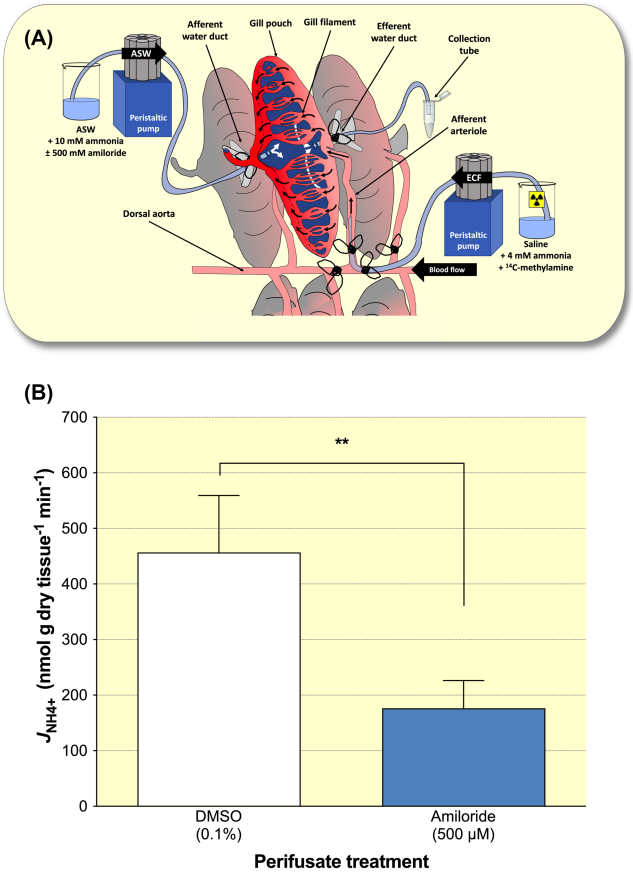


FIGURE 5 Amiloride reduces unidirectional J_{NH4+} in a novel dual perfusion/perifusion in situ gill pouch preparation. (A) schematic of dual perfusion/perifusion preparation. (B) unidirectional J_{NH4+} was measured as the appearance of ^{14}C-MA from blood to water, accounting for the ^{14}C-MA: NH_4^+ specific activity (*see methods*) in isolated gill pouches of hagfish pre-exposed to HEA (10 mmol/L) for 24 h were carried out. J_{NH4+} was determined in the absence and presence of amiloride (500 μM). $p < 0.05$; one-tailed repeated measures Student's t-test. $n = 7$.

2.6 | Experiment 6: Gill Rh protein expression and sub-cellular localization in response to HEA exposure

Western blotting revealed that gill samples from hagfish exposed to HEA for 24 h had roughly half the Rh channel protein abundance compared to control animals (Figure 6; $p = 0.0230$). To further investigate the significance of this down-regulation, Rh channel and NKA were immunolocalized and visualized using confocal microscopy. In gills from control hagfish, a very intense NKA signal was evident in cuboidal cells in contact with seawater (Figure 7A); these cells are the ionocytes, and the punctate pattern reflects NKA localization in their highly in-folded basolateral membrane.[4] On the other hand, the Rh signal was widespread throughout the gill tissue (Figure 7B). 3D confocal reconstructions revealed the distinct presence of Rh channel in the apical membrane of NKA-rich ionocytes and on the basolateral membrane of the pavement cells (Figure 7D–F). Consistent with the Western blotting results, gills from HEA-exposed hagfish had qualitatively dimmer overall Rh signal. However, the most striking finding was the disappearance of Rh channel from the apical membrane of NKA-rich ionocytes (Figure 7G–I).

3 | DISCUSSION

In this study, we demonstrated the outstanding ability of hagfish to hypo-regulate T_{amm} in their plasma in the face of substantial inwardly direct gradients of both NH_4^+ and NH_3. Furthermore, multiple lines of evidence indicate that hypo-regulation of plasma ammonia is mediated by active excretion of NH_4^+ through apical NHEs in the gill

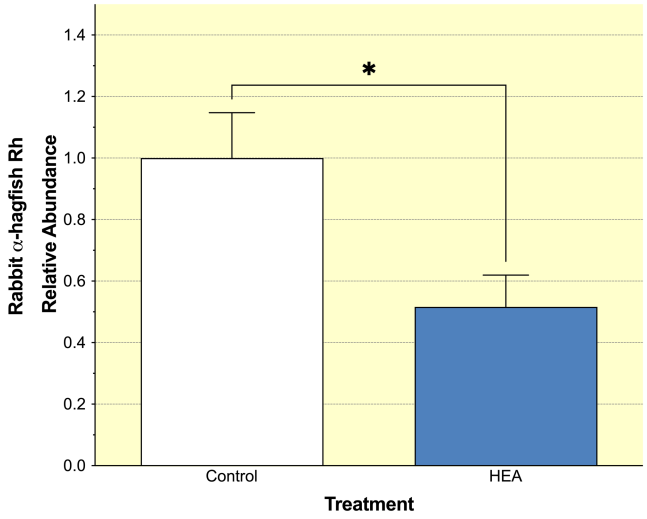


FIGURE 6 anti-hagfish Rh abundance in gill homogenates from control and HEA-exposed hagfish (10 mM NH_4Cl, 24 h). Abundance was normalized to control samples within each fraction. The letters denote significant differences ($p < 0.05$; one-tailed repeated measures Student's t-test.). $n = 6$.

NKA-rich ionocytes. Moreover, removal of Rh channels from the apical membrane of these gill ionocytes likely acts to reduce ammonia loading during HEA thus contributing to plasma ammonia hypo-regulation.

3.1 | Ammonia generation during marine decomposition

Hagfish are necrophages who routinely enter into putrefying carcasses to feed.[1] In terrestrial environments, T_{amm} levels in the soil surrounding a decomposing carcass can reach ~30 mmol kg^{-1}.[36] However, the chemistry within carcasses lying on the ocean's floor remains unknown due to the considerable difficulty in obtaining such data. To estimate the magnitude of HEA as a result of putrefaction within a whale carcass, we placed bovine muscle and liver tissue in unfiltered seawater and measured $[T_{amm}]_w$ throughout a 17-day incubation period at 12°C. The increase in $[T_{amm}]_w$ during decomposition was steep for both tissues, exceeding 7 mM $[T_{amm}]_w$ after just 24 h, 50 mM after 4d, and approaching 100 mM after 17 days (Figure 1A). We also noted that tissue decomposition led to the generation of $[H^+]$ and pCO_2 resulting in a highly acidic and hypercapnic environment, especially in the later stages of the experiment.

Clearly, tissue rotting in a sealed syringe does not completely match the interior of a putrefying whale carcass, which is expected to have some degree of connectivity with the environment and ensuing water turnover. Nonetheless, these measurements demonstrate that bacterial decomposition of mammalian tissue in seawater can result in HEA and hypercapnia. Although not measured in our experiments, putrefaction is bound to also deplete O_2 leading to hypoxia or anoxia, and perhaps produce other compounds such as hydrogen sulfide. These extreme conditions are likely to have shaped the high tolerance of hagfishes to pH [6,7,14–17] and ammonia disturbances.[8,9,23]

Interestingly, tissue decomposition induced seawater acidification down to pH ~6 after 12 h (Figure 1A). The pNH_3 gradient at the apical interface of the gill ionocytes is dependent on both $[T_{amm}]$ and pH in the ionocytes and seawater; the noted lower seawater pH would theoretically facilitate the renewal of net NH_3 diffusion, thus raising the question of whether active ammonia excretion would be necessary. The direction of NH_3 diffusion is fundamentally dictated by the ΔpNH_3 gradient such that diffusion out of the animal will occur only when:

$$pNH_{3i} > pNH_{3o}. \quad (1)$$

To determine the theoretical limits of passive NH_3 diffusion in a control hagfish ($[T_{amm}]_p$ = 50 μM), ΔpNH_3 was modeled across an increasing $[T_{amm}]_o$, and along different pH_i (pH 7.0, 8.0) and pH_o (pH 5.0–8.0) values (Figure 8), which we used to determine the NH_3/NH_4^+ speciation (see calculations). By so doing, we see that at pH_o values observed by 24 h of decomposition (pH ~6.0), we would indeed expect a reversal of the ΔpNH_3 gradient upon introduction of a control hagfish to any $[T_{amm}]_o$ beyond 0.5–5 mM (bounded by pHi 7.0–8.0).

For the purposes of this study, we chose to focus our investigations on the effect of high ammonia in isolation from low pH and high pCO_2; however, given the large accumulations of CO_2 and ammonia generated during the decomposition, future studies should aim to understand the combined effects of HEA, hypercapnia and hypoxia in hagfish, while also aim to better understand putrefaction in marine environments.

3.2 | Regulation of $[T_{amm}]_p$ during HEA exposure

Based on the $[T_{amm}]_w$ observed in the in vitro decomposition study, we exposed hagfish to 1–20 mM $[T_{amm}]_w$ HEA for 48 h, concentrations that seem attainable inside a decomposing whale carcass in a 48 h timeframe. These HEA conditions entail pronounced and persistent inwardly directed NH_3 and NH_4^+ gradients (Figures 2B,C and 8). If hagfish lacked the ability to actively excrete NH_4^+, $[T_{amm}]_p$ would accumulate to levels above the environmental concentrations until reaching a level that restores net outward pNH_3, as has been observed in sea lamprey exposed to HEA (*Petromyzon marinus*).[37]

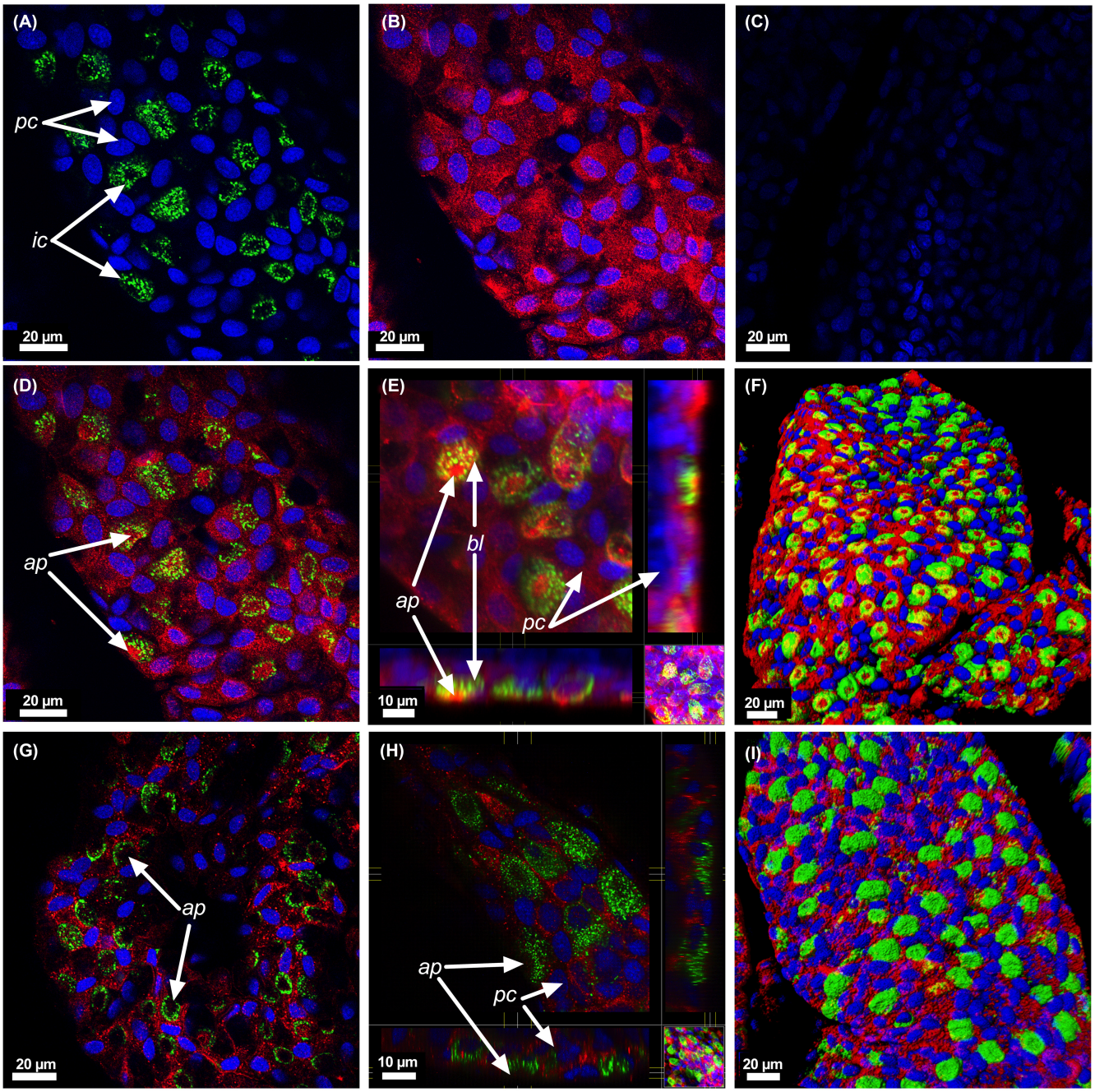


FIGURE 7 HEA exposure elicits removal of Rh channels from the apical membrane of gill ionocytes. Representative Imaris-processed, whole-mount confocal (A–D, G), *z*-stack orthogonal-projection (E, H), and 3D volume-filled reconstruction (F, I) images of hagfish gill filaments immuno-stained with anti-hagfish Rh (red) and monoclonal NKA (green) antibodies, nuclei were stained with DAPI (blue). (A) NKA (B) Rh and (C) no-1° antibody control images of gill filaments from a control hagfish showing individual staining patterns of each channel. In (E, H) bottom and right-hand sub-panels show *x, z* and *y, z* dimensions while lower right panel shows maximum intensity projection. Apical (*ap*) and basolateral (*bl*) regions of NKA-rich ionocytes (*ic*) and pavement cells (*pc*) are indicated. $n = 3$.

To illustrate this, we again modeled ΔpNH_3 across different pHi and pHo values, this time holding $[T_{amm}]_o$ bound to 10 000 µM across increasing $[T_{amm}]_i$, in essence mimicking ammonia loading into an animal during HEA onset (Figure 8B). From this, we can see that the pH of the experimental water used throughout our experiments essentially removed any capacity for passive NH_3 excretion. Nevertheless, $[T_{amm}]_p$ consistently equilibrated in HEA-exposed hagfish at levels that were 20%–25% of those found in the seawater (Figure 1A).

Since hagfish do not increase the production of nitrogen-containing metabolites during exposure to HEA,[9] we hypothesized that hagfish are either able to reduce their diffusive permeability to exogenous ammonia,

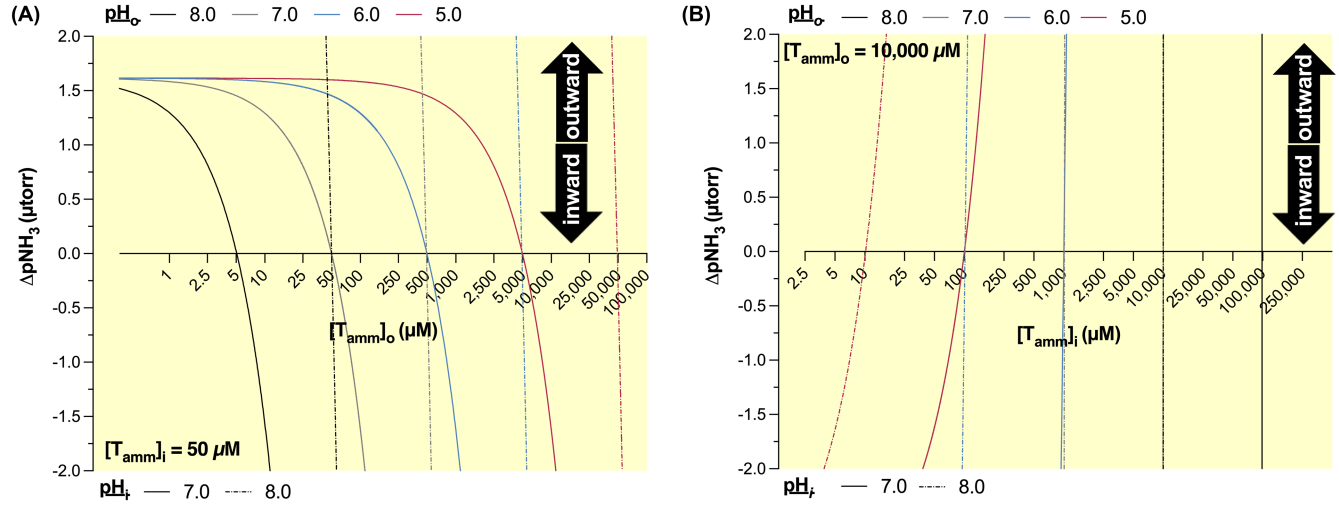


FIGURE 8 Thermodynamic modeling pNH_3 gradients. The influence of pHo and either (A) environmental $[NH_4^+]$ or (B) intracellular $[NH_4^+]$ on the relative ΔpNH_3 transport direction. Each curve represents a different pHo as illustrated in the figure legend. Panel (A) mimics a control hagfish with an $[T_{amm}]_i$ of 50 μM and can be used to predict the $[T_{amm}]_o$ where loss of net diffusion would occur. Panel (B) mimics a hagfish held in 10 mM HEA conditions and can be used to identify the $[T_{amm}]_i$ that would need to be realized at a given pHo to restore the net pNH_3 excretion gradient. The effect of pHi is also plotted (Solid lines: pHi = 8.0; hatched lines: pHi = 7.0).

actively excrete NH_4^+ against an inwardly directed gradient, or both. Incidentally, from our model, we can also see that any hagfish entering a hypothetical 10 mM HEA/pH 6.0 environment, conditions paralleling those observed during our marine decomposition study, would not be able to re-establish an outwardly directed pNH_3 gradient until accumulating ~100 μM–1 mM $[T_{amm}]_p$, dependent on pHi.

3.3 | Determination of a role for environmental Na^+ in the stabilization of $[T_{amm}]_p$ and active excretion of NH_4^+ during HEA exposure

Our experiments utilizing altered water chemistries revealed the importance of environmental Na^+ in hagfish ammonia handling during HEA exposure. Following an initial 24 h pre-exposure to 10 mM HEA, continued exposure to HEA in Na^+-free conditions significantly impaired the ability of hagfish to hypo-regulate $[T_{amm}]_p$ during the subsequent 5 h of continued HEA exposure (Figure 3A). This impairment was associated with a progressive blood acidosis (Figure 3B), which would be expected under the circumstances; the reversal of the Na^+ gradient in Na^+-free conditions would attenuate apical NHEs, thus generating an H^+ backlog within the organism. These results provided strong evidence for the involvement of an underlying Na^+-linked mechanism in hagfish ammonia regulation.

To establish whether hagfish are indeed able to actively excrete ammonia against a 10 mM HEA background, we used the NH_4^+ analog, ^{14}C-MA, as a proxy tracer for ammonia excretion. This analog has been previously validated to estimate NH_4^+ fluxes across a diversity of membranes and tissue types including cyanobacteria,[38] mammalian renal tubule,[39] and invertebrate and vertebrate gills.[40,41] Impressively, HEA exposed animals exhibited a 220-fold greater net outward NH_4^+ flux compared to control animals (Figure 4), reflecting an upregulation in NH_4^+ excretion capacity and corroborating the presence of an active NH_4^+ excretion mechanism. Furthermore, continued exposure to HEA in Na^+-free medium drastically attenuated active ammonia excretion. The residual J_{NH4+} observed in the nominally Na^+ free condition (~100 μmol kg^{-1} h^{-1}) is likely due to an inability to eliminate Na^+ from the bathing media due to Na^+ efflux from the animal when placed in Na^+-free seawater. Overall, these results suggest a Na^+-dependent mechanism for active ammonia excretion, leading us to explore the potential role of NHEs in excreting NH_4^+ in exchange for external Na^+.

3.4 | NHE-dependent active NH_4^+ excretion across hagfish gills during HEA exposure

A pharmacological hallmark for the involvement of NHEs is inhibition by amiloride.[42] However, pharmacological inhibition in whole-animal experiments can be difficult to interpret due to the presence of NHEs in multiple tissues. To overcome these limitations, we developed an in situ double perfusion technique for hagfish gill pouches and examined the effect of amiloride on J_{NH4+} excretion in gills of hagfish previously exposed to HEA (Figure 5A). These isolated and perfused/perifused

hagfish gill pouches demonstrated active and outwardly directed J_{NH4+} (Figure 5B) that was amiloride-sensitive. To this end, amiloride impaired J_{NH4+} by ~60%, demonstrating a clear amiloride-sensitive component to active NH_4 excretion. This incomplete inhibition may be in part due to the possibility that hagfish NHE(s) differ in their pharmacological sensitivity to amiloride; indeed, recent work with heterologously expressed teleost NHEs demonstrates a greater resiliency to amiloride compared to mammalian NHEs.[43] Alternatively, there could be a lower level of bioavailable amiloride in the high ionic strength seawater, resulting in decreased pharmacological inhibition. Nevertheless, the noted amiloride-sensitivity in the perfused gill experiment strongly supports the observations of active NH_4^+ excretion in our whole-animal studies (Figure 3), but also suggests that regulation and active excretion is critically reliant on an NHE-dependent mechanism in hagfish gill ionocytes.

NHEs are bi-directional transporters whose direction is dictated by environmental and intra-ionocyte concentration gradients of $[Na^+]$ and $[H^+]$, such that Na^+ uptake and H^+ excretion take place when

$$\frac{[Na^+]_i}{[Na^+]_o} < \frac{[H^+]_i}{[H^+]_o} \quad (2)$$

is true.[44–46] It is important to note that modeling of an $Na^+/H^+(NH_4^+)$ mechanism would rely on both intracellular and extracellular pH, $[Na^+]$ and $[NH_4^+]$ and Equation (1) can be modified to incorporate these factors. NHE-mediated NH_4^+ excretion would thus be predicted to occur when

$$\frac{[Na^+]_i}{[Na^+]_o} < \frac{[H^+]_i + [NH_4^+]_i}{[H^+]_o + [NH_4^+]_o}; \quad (3)$$

however, in addition to a lack of available measurements of intra-ionocyte $[Na^+]$, pH, and $[NH_4^+]$ in both control and HEA hagfish, critical features of this model, such as relative affinity constants for each of the substrates remain to be elucidated through the use of two substrate kinetics.[47]

3.5 | Rh channel sub-cellular redistribution within gill ionocytes during HEA exposure

Given the data presented thus far, two mechanistic models can be postulated to allow NHEs to actively excrete NH_4^+ against persistent inwardly directed gradients. One option is acid-trapping using an apical NHE operating in conjunction with an apical Rh channel. The NHE would supply H^+ and acidify Rh-mediated NH_3 into NH_4^+at the apical boundary layer, thus providing a persistent outwardly directed gradient for continued diffusion of NH_3. However, the presence of an apical Rh during HEA exposure could allow back-flux of NH_3 into the animal, thus short-circuiting active net ammonia excretion. Alternatively, NH_4^+ could be directly excreted via the apical NHE, through secondary active transport energized by the activity of basolateral NKA. Notably, this mechanism does not require an associated apical Rh channel.

To investigate the expression of Rh channels in active ammonium excretion and $[T_{amm}]_p$ regulation during HEA exposure, we quantified Rh channel protein abundance by Western blotting and further determined the sub-cellular localization of Rh channels in hagfish gills using immunohistochemistry, confocal resolution microscopy, and Z-stack image reconstructions. Homogenates of gills from 24 h HEA-exposed hagfish had roughly half the Rh channel abundance compared to control animals (Figure 6, Figure S1A).

The peptide to which our hagfish Rh antibody was raised cannot discriminate between Rhcg (the apical Rh isoform) and Rhbg (the basolateral Rh isoform) (Table 3); however, our immunohistochemical analysis with the Rh antibodies yielded clear staining patterns from which to draw inference. Our microscopy demonstrated that during control conditions, Rh signal was densely localized on the apical membrane (Figure 7) of ionocytes, indicative of their role in diffusion-based NH_3 excretion during routine conditions. We also noted dense basolateral staining on both pavement cells (which lacked any discernible apical staining) and ionocytes. Here the role of Rh would be to facilitate transport of ammonia produced metabolically

TABLE 3 Comparison of antibody epitopes used for Westerns and immunocytochemistry

Myxine glutinosa Rh epitope	C	Y	E	D	R	A	Y	W	E	V	P	E	E	E	V	T	Y
Eptatretus stoutii Rhcg	C	Y	E	D	E	A	Y	W	E	V	P	E	E	E	V	T	L
Eptatretus stoutii Rhbg	C	F	E	D	S	M	Y	W	E	V	P	E	A	E	-	G	F

Note: The epitope sequences of the polyclonal anti-Atlantic hagfish (*Myxine glutinosa*) Rhcg antibody aligned against previously characterized *E. stoutii* Rhbg and Rhcg isoforms.[26] Homologous amino acid residues are highlighted in bold. The anti-Atlantic hagfish Rhcg antibody shared an 88% sequence identity to Pacific hagfish Rhcg and 65% sequence identity to Pacific hagfish Rhbg.

from within the pavement cell to the blood and/or directly to the ionocytes. However, following HEA exposure, apical staining of Rh signal on the ionocytes was strikingly absent. We also observed a more muted Rh staining pattern in the basolateral membranes of both the ionocytes and the pavement cells (Figure 7F–H). Thus, by using established patterns of Rh isoform localization,[21] our results suggest that shuttling of an apical Rhcg out of the apical membrane, and reduction of Rhbg from the basolateral membrane are essential branchial re-modeling mechanisms for hypo-regulation of plasma T_{amm}.

Overall, these results agree with the reductions in protein expression observed via Western blotting and together they strongly argue against the involvement of an apical Rh channel in the active excretion of NH_4^+, and thus against an acid-trapping mechanism. Removal of an apical Rh further supports our hypothesis that a critical aspect of hagfish HEA tolerance is a reduction in gill permeability to NH_3 and points to the use of a Na^+/NH_4^+ exchange as the mechanism underlying active J_{NH4+} excretion.

Based on these immunological observations, we propose a model in which the mode of Rh-mediated ammonia excretion is plastic, depending on the concentrations of ammonia in the water. Given the pH-dependency of NH_3/NH_4^+ speciation (pKa ~ 9.3), during control conditions when blood pH is ~8.0 and when concentrations of environmental and plasma ammonia are relatively low, entry of metabolically generated ammonia from the blood into the ionocytes primarily occurs via diffusive NH_3 transport through the abundance of Rhbg on the basolateral membrane of ionocytes (Figure 9A). The observed Rhbg expression in the pavement cells likely facilitates offloading of metabolically produced ammonia into the nearby ionocytes and/or the interstitial fluid. At the apical surface of the ionocytes, ammonia is subsequently excreted into seawater by diffusion via apical Rhcg channels. While minimal at this physiological pH, NH_4^+ can also transport across the basolateral membrane of the ionocytes through NKA activity, K^+-dependent Cl^- cotransporters (i.e. NKCC and KCC transporters) and K^+ channels, owing to the fact that NH_4^+ and K^+ share nearly identical hydration shell sizes, ionic conductance, and water mobility rates.[48,49]

During early exposure to HEA, the NH_3 diffusive gradient is inwardly directed, so an apical Rhcg would allow for persistent ammonia loading and short-circuit net ammonia efflux (Figure. 9B). Consequently, the observed removal of Rhcg from the apical membrane of gill ionocytes would serve to reduce diffusive ammonia loading (Figure 9C). By reducing apical Rhcg abundance in response to HEA, the animal is left with a reduced permeability for ammonia across the apical membrane, leaving the animal unable to utilize passive ammonia excretion, at least until both the restoration of passive excretion is thermodynamically favorable and more importantly, there is a restoration of apical Rhcg expression. The utility of alternative K^+-based, basolateral NH_4^+ transport pathways may play a more prominent role following ammonia accumulation when $[NH_4^+]_p$ increases

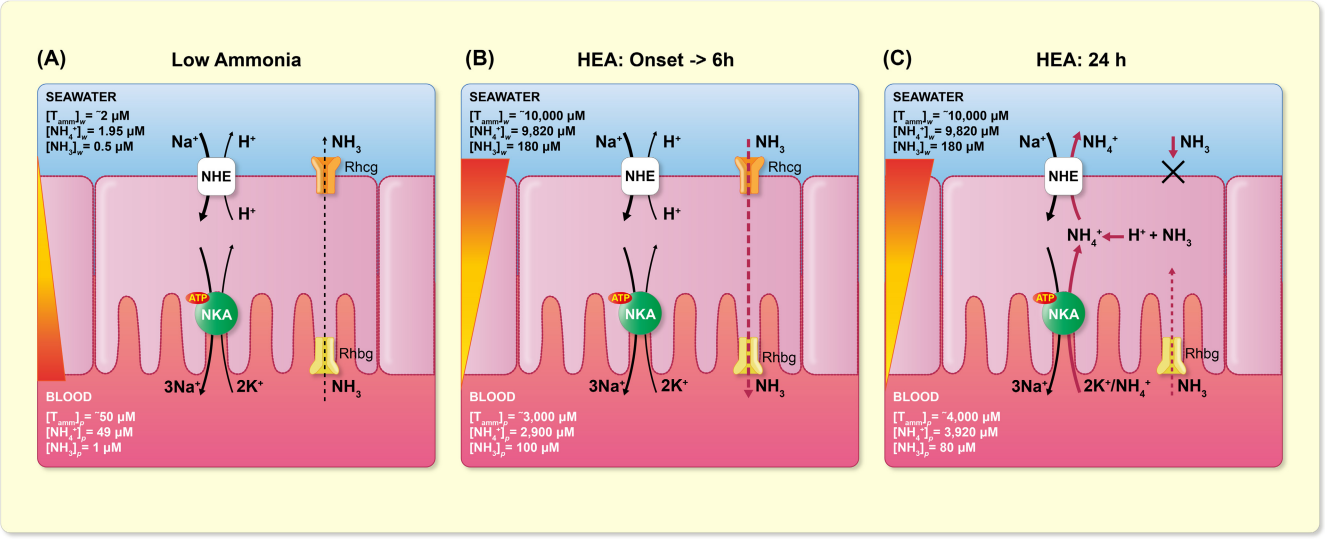


FIGURE 9 Proposed models for ammonia excretion in hagfish gill ionocytes during exposure to control and HEA conditions. Rhbg/Rhcg, Rhesus glycoprotein; NHE, Na^+/H^+ exchanger; NKA, Na^+/K^+-ATPase. (A) During routine (low ammonia) conditions, ammonia is excreted primarily as NH_3 across gill epithelia via basolateral Rhbg and apical Rhcg ammonia channels, moving along outwardly directed ammonia driving gradients. (B) During exposure to HEA (10 mM; 0–6 h), ammonia driving gradients shift inwards, causing accumulation of ammonia via the gradient driven ammonia channels. (C) After 24 h, $[T_{amm}]_p$ accumulation stabilizes below $[T_{amm}]_w$, which is associated with a removal of Rhcg from the apical membrane, and active excretion of NH_4^+ via amiloride-sensitive NHE driven by favorable Na^+ gradients.

and future studies should seek to understand the roles of these transporters in hagfish during HEA exposure.

3.6 | Summary, conclusions, and perspectives

The multiple lines of evidence presented in this study indicate the presence of an NHE-dependent mechanism in hagfish gills which allows hagfish to actively excrete NH_4^+ during exposure to HEA. Moreover, decreased abundance of Rh channels at the apical membrane of ionocytes serves to reduce diffusive NH_3 influx and prevents short-circuiting of NHE-mediated NH_4^+ excretion. In combination, these responses contribute to the ability of hagfish to maintain their plasma ammonia concentrations well below that of the high ammonia environment. Together with their exceptional tolerance to hypoxia and hypercapnia, the active ammonia excreting mechanism identified in our study allow hagfish to exploit the nutrient-dense environment found inside a decomposing whale carcass, which would be toxic or fatal to most other marine animals. The ancestral lineage of hagfishes has persisted for over 500 million years following their divergence from the rest of the vertebrate lineage[50]; the flexibility in nutritional sources afforded by the adaptations described herein likely gave ancestral hagfish a selective advantage contributing to their evolutionary success.

4 | MATERIALS AND METHODS

4.1 | Experimental animals and husbandry

Hagfish (*Eptatretus stoutii*; ~50–150 g) were captured using baited hagfish pots from either Trevor Channel (Bamfield, BC, Canada) or off the coast of La Jolla (CA, USA). In each location, hagfish were held in 200 L tanks continuously receiving sea water ($T = 12 \pm 1°C$), fed biweekly with decomposing hake, and fasted for a minimum of two weeks prior to experimentation. Experiments were performed at the Bamfield Marine Sciences Centre (BMSC) under protocols approved by the BMSC Animal Care Committee and adhered to Canadian Council for Animal Care guidelines, or at Scripps Institution of Oceanography – UCSD, following Institutional Animal Care and Use Committee (IUCAC) guidelines.

4.2 | Chemicals

Tricaine methanesulfonate (TMS) was obtained from Syndel laboratories (Nanaimo, BC, Canada).^{14}C-MA was sourced from ViTrax (Placentia, CA). Unless otherwise specified, all other reagents were obtained from Sigma–Aldrich Chemical Company (St. Louis, MO).

4.3 | Experimental protocols

Prior to all experimental series, hagfish were acclimated overnight in 22 L chambers continuously receiving well-aerated sea water (flow rate ~1 L/min). All whole-animal experiments were conducted in water held at 12°C; in situ experiments were conducted at room temperature (~16–18°C) for practicality.

4.3.1 | Experiment 1: Determination of ammonia generation, acid–base, and pCO_2 dynamics during marine decomposition

Bovine (*Bos taurus*) muscle and liver tissues were obtained from local butcher shop and portioned into 1 g masses of tissue ($n = 3$ for each tissue). Tissues were blotted, weighed, then placed along with a small stir-bar into 50 ml syringes with plungers removed (flux chambers). The plungers were replaced, and the dry weight of the chambers was measured. Chambers were then filled with unfiltered natural seawater (35 ppt) such that there was no dead-space, and an initial water sample (1 ml) was taken. A set of chambers were also prepared in the same manner without any tissue added (tissue-free controls). Chambers were then sealed, and the weight of the chamber was measured again to calculate water volume. Chambers were placed into a water-bath held at 12°C for up to 17 days. At intermittent time points, chambers were removed from the water-bath, stirred and then sampled for water (1 ml). Water samples were drawn from the chamber in a manner that prevented any accumulation of dead-space (from bacterial respiration) from leaving the chamber. Water samples were immediately frozen for later determination of total water ammonia $[T_{amm}]_w$.

4.3.2 | Experiment 2: Determination of $[T_{amm}]_p$ regulation during HEA exposure

Pacific hagfish ($n = 36$) were transferred from holding tanks to 22 L experimental chambers receiving flow-through seawater and aeration in groups of 3 animals per chamber and were acclimated overnight to lab conditions. Following acclimation, flow-through conditions were stopped, water volumes adjusted to 20 L and sufficient NH_4Cl solution was added to each chamber to yield a final $[T_{amm}]_w$ of 0, 1, 2, 5, 10, and 20 mM (6 animals per

exposure concentration). At regular time intervals (6, 12, 24, 48 h), hagfish were anesthetized one chamber at a time by carefully transferring animals to a separate container containing neutralized tricaine methanesulfonate (0.5 g/L TMS + 0.15 g/L NaOH) in seawater and the appropriate concentration of NH_4Cl. This dose of TMS caused rapid, relatively shallow sedation (<5 min) from which the hagfish rapidly recovered (<5 min), and prevented slime production during handling.[15] Upon anesthetization hagfish were held vertically to promote pooling of blood in the caudal sinus from which a blood sample (250 µl) was drawn using a 23-gauge needle and syringe pre-rinsed with heparinized saline (50 U Na-heparin ml^{-1} in 0.5 M NaCl). The pH of the whole blood sample was then determined, and the remainder centrifuged at 10 000*g* for 2 min, with the resultant plasma supernatant drawn off and immediately frozen for subsequent determination of $[T_{amm}]_p$. Each hagfish was then immediately returned to exposure chambers until the next designated sampling period. All hagfish were sampled for blood at each timepoint; however, given the design of the experiment, samples were unable to be tracked on a repeated measures basis.

4.3.3 | Experiment 3: Determination of a role for environmental Na^+ in the stabilization of $[T_{amm}]_p$ during HEA exposure

This series of experiments examined the role of environmental Na^+ on the ability of hagfish to hypo-regulate their plasma ammonia levels. After exposure to HEA (10 mM NH_4Cl) for 24 h, hagfish ($n = 14$) were anesthetized, blood was collected, and hagfish were transferred to a second set of chambers (500 ml) with HEA in either normal seawater or Na^+-free artificial seawater (in mM: Choline 484; Cl^- 570.0; Mg^{2+} 56.0; SO_4^{2-} 29; Ca^{2+} 11; K^+ 9.0; HCO_3^- 2.1; adjusted to pH 8.0 with KOH). Repeated blood samples (250 µl) were collected at 1, 2.5 and 5 h from each animal and frozen for later determination of $[T_{amm}]_p$.

4.3.4 | Experiment 4: Determination of active and Na^+-dependent NH_4^+ excretion during HEA exposure

The fourth series of experiments examined the capacity for hagfish to actively excrete ammonia and to determine the role of environmental Na^+ on potential active excretion mechanisms. Hagfish were exposed to either control or HEA (addition of 10 mM NH_4Cl in seawater) conditions for an initial 18 h of exposure, anesthetized (as above), and injected (caudle sinus) with ^{14}C-MA (0.025 µCi g^{-1} animal in 2.5 µl hagfish saline g^{-1} animal) as a radio-labeled proxy for NH_4^+. Hagfish were then gently inverted several times to promote mixing and immediately returned to the control or HEA condition for an additional 6 h to allow the ^{14}C-MA to evenly distribute throughout the body. At 24 h of total HEA exposure, hagfish were anesthetized and held vertically to promote blood pooling in the caudal sinus, from which a blood sample (250 µl) was drawn using a 23-gauge needle and syringe pre-rinsed with heparinized saline (50 U Na-heparin/ml in 0.5 M NaCl). After blood sampling, control and HEA-exposed hagfish from each pre-treatment were immediately transferred to individual flux chambers (500 ml) containing 10 mM NH_4Cl in either artificial seawater (ASW; in mM: Na^+ 455.4; Cl^- 482.7; Mg^{2+} 48.2; SO_4^{2-} 48.2; Ca^{2+} 10.2; K^+ 9.4; HCO_3^- 2.5; pH 8.0) or Na^+-free artificial seawater (in mM: N-Methyl-D-Glucamine (NMDG) 455.4; Cl^- 482.7; Mg^{2+} 48.2; SO_4^{2-} 48.2; Ca^{2+} 10.2; K^+ 9.4; HCO_3^- 2.5; pH 8.0 adjusted with HCl). Water samples (~6 ml) were collected immediately and after 2.5 h of exposure for measurement of total water ammonia ($[T_{amm}]_w$), at which time the hagfish were euthanized (5 g/L MS222 + 1.5 g/L NaOH in seawater or HEA-seawater) and a second blood sample collected. Blood and water samples were examined immediately for determination of pH. Blood was then centrifuged to obtain plasma supernatant, which along with water samples, were subsampled (30 µl plasma, 5 ml water) for determination of ^{14}C-MA activity, and the remaining sample frozen for later determination of water and plasma $[T_{amm}]$.

4.3.5 | Experiment 5: Effect of Na^+/H^+ transport inhibition on apparent NH_4^+ excretion in a perfused gill pouch model

To corroborate the gill as the site of active ammonia excretion, and interrogate a possible role for NHE, we conducted a series of ^{14}C-flux experiments with an isolated in situ hagfish gill perfusion preparation. Following acclimation and subsequent exposure to HEA for 24 h, hagfish were anesthetized (as above), injected with a bolus of heparinized saline (5 U heparin / g fish, as 1 U Heparin/µl in 500 mM NaCl) to prevent clotting, inverted several times to promote mixing of the blood, and euthanized. Hagfish were then blotted dry, and a ventral incision was made between the 1st and 8th branchiopores. Adipose and connective tissue surrounding the 3rd, 4th and 5th gill pouches was removed to expose the dorsal aorta, the afferent arterioles, and the corresponding afferent and efferent water ducts.

An individual gill pouch was then isolated and prepared for dual perfusion/perifusion based on the

protocol described by Forster and Fenwick[51] in broadgill hagfish (*Eptatretus cirrhatus*). However, the much smaller size of *E. stoutii* (~50–150 g) relative to *E. cirrhatus* (~1 kg) required some modifications including reductions in tubing size and reduced flow rates. The afferent and efferent water ducts and the afferent arteriole for the 4th left gill pouch were cannulated with PE50 tubing that was either flared (water ducts) or pulled over a flame to ~PE20 (afferent arteriole). Since there are no known flow rates for *E. stoutii* gill vasculature, preliminary experiments were used to define perfusion flow rates that had similar blood pressures when compared to normal hagfish blood pressure (~13 cm H_2O/1 mmHg) and these perfusion rates were validated by testing for >120 min while observing for consistent excretion rates. These flow rates also allowed for enough time for isotopic exchange to occur within a 15 min window. Preparations where epithelial integrity failed were easily detected, as when tissue rupture occurred, it would result in the sudden release of the radioactive perfusate into the perifusate, and result in very high sample counts.

The water duct was perifused with ASW spiked with 10 mM NH_4Cl at a rate of 0.13 ml/min, while the afferent arteriole was perfused with hagfish ringers (in mM: NaCl 474; KCl 8; $CaCl_2$ 5; $MgSO_4$ 3; MgCl2 9; NaH_2PO_4 2.06; $NaHCO_3$ 5; pH 7.9) spiked with 4 mM NH_4Cl and ^{14}C-MA (0.2 μCi/ml) at a rate of 0.02 ml/min at room temperature.

Successful perfusion of the gill pouch blood vessels was visualized by adding household blue food coloring into the perfusate (Figure 3A; Video S1). After passing through the gill pouch, the perifusate was collected for later analysis of ^{14}C-MA radioactivity. Gill pouch preparations were allowed to flush for 15 min, followed by the collection of perifusate in two successive 15-minute measurement periods. Initial preparations demonstrated that tissue preparations provided stable J_{NH4+} measurements over the course of at least 120 min without loss of preparation integrity. Leaks and faulty preparations were easily identified by the appearance of large number of ^{14}C-MA counts in the final perifusate that were of similar magnitude to the perfusate (~550 CPM μl^{-1} in 100 μl perfusate) and well beyond what was observed perifusate samples from patent preparations (2–16 CPM μl^{-1} in 500 μl final perifusate). To explore the involvement of NHEs in ammonia excretion, the perifusate was switched to ASW containing 500 μM amiloride and collected as described above. This concentration was chosen based on recent studies demonstrating that some freshwater teleost NHEs are not inhibited by amiloride below 500 μM.[43,52]

4.3.6 | Experiment 6: determination of gill Rh protein expression and sub-cellular localization in response to HEA exposure

In a final series of experiments, hagfish were euthanatized after exposure to HEA (10 mM for 24 h), dissected and gill pouches were excised and either immediately flash frozen for Western blotting, or fixed in ice-cold fixative [(4%-paraformaldehyde in phosphate buffer saline (PBS)] for 8 h for immunohistochemistry. Fixed gill pouches were incubated (30 min) first in 50%, then 70% ethanol and stored at 4°C.

4.4 | Analytical techniques

4.4.1 | Water and blood acid–base and ammonia measurements

Water and blood pH were measured immediately using a thermo-jacketed (10 °C) Orion ROSS micro pH electrode (Fisher Scientific, Ottawa, ON). Blood samples were then centrifuged at 10 000 *g* for 2 min to obtain a plasma supernatant. An aliquot of plasma was drawn-off and analyzed for total CO_2 (TCO_2) using a Corning 965 carbon dioxide analyzer (Ciba Corning Diagnostic, Halstead, Essex, UK) while the remainder was immediately frozen for subsequent determination of plasma total ammonia concentration ($[T_{amm}]_p$) using a commercially available kit (Sigma-Aldrich Procedure A001) at 340 nm. Water samples were analyzed for $[T_{amm}]_w$ via colorimetric determination using the salicylate-hypochlorite assay at 650 nm[53] with a microplate spectrophotometer (Spectramax 190, Molecular Devices, Sunnyvale, CA) as previously described.[9] Due to protein interference, water samples generated in Experiment 1 were analyzed for $[T_{amm}]_w$ with a commercially available fluorometric ammonia assay (Sigma, MAK310). Blood and water pH and $[T_{amm}]$ were utilized to calculate NH_3 and NH_4^+ based on the Henderson-Hasselbalch equation.[54] Measured values of blood and water pH and TCO_2 were used to calculate pCO_2 at 12°C by the Henderson–Hasselbalch equation, using the general formulas for pK_{app} and αCO_2 derived by Heisler and cited in Boutilier et al.[55]

4.4.2 | Measurements of ^{14}C-MA radioactivity

Water (5 ml), plasma (30 μl), perfusate (100 μl pre-perfusion), and perifusate (500 μl post-perifusion) samples containing ^{14}C-MA were mixed with 5 ml of liquid scintillation fluor (Optiphase Hisafe 2 scintillation cocktail,

PerkinElmer, MA, USA) and left overnight to minimize chemiluminescence. Samples were thereafter measured for beta radioactivity (LS6500; Beckman Coulter, California).

4.4.3 | Antibodies for immunological detection

The Western blotting and immunohistochemistry experiments utilized previously developed rabbit anti-Atlantic hagfish (*Myxine glutinosa*) Rh antibodies raised against the peptide CYEDRAYWEVPEEEVTY.[23] This amino acid sequence is highly conserved in hagfish Rhcg and Rhbg[26] (Table 3), and therefore the anti-hagfish Rh antibodies can be expected to immunodetect both isoforms.

A mouse monoclonal antibody against the α-subunit of chicken NKA (Developmental Studies Hybridoma Bank[57]) was used to immunodetect hagfish NKA by immunohistochemistry and identify gill ionocytes. This antibody is routinely used to immunodetect NKA in fish gills, including hagfish.[4,8]

4.4.4 | Western blotting

Frozen gill pouches were processed to obtain protein homogenates as previously described.[17,58] Protein concentration was assayed on homogenized aliquots using a Bradford-based assay (Bio-Rad Laboratories, Inc., USA). Samples were thereafter diluted with homogenization buffer to 1 μg/μl protein concentration, combined with 4X Laemmli buffer (Bio-Rad) and heated (70°C, 15 min). 10 μl of each sample was loaded into 0.1% SDS/10% polyacrylamide mini-gels and electrophoresed for 1 h at 200 V. Separated proteins were wet-transferred to a PVDF membrane (12 h at 90 mAmps, 4°C) and incubated in blocking buffer [0.5 M Tris-buffered saline with 0.1% Tween, pH 8.0 (TBST) containing 10% skim milk powder] (room temperature, 15 min) before incubation with the anti-hagfish Rh antibodies (312.5 ng/ml in blocking buffer, room temperature, 2 h). Membranes were then washed in TBST (3 × 5 min) and incubated with HRP-conjugated goat anti-rabbit antibodies (15 000 in blocking buffer, room temperature, 2 h). Finally, membranes were washed in TBST (4 × 5 min), and bands were made visible through the addition of enhanced chemiluminescence/peroxide substrate (Bio-Rad) and subsequently imaged on the Bio-Rad Universal III Chem-doc system using 'Image Lab' software (version 6.0.1; BioRad). The anti-hagfish Rh antibodies yielded a single band at ~50 kDa in all fractions (Figure S1A). The PVDF membrane was incubated in Ponceau stain (5 min, room temperature) and imaged to estimate protein loading (Figure S1B). Relative protein abundance ($n = 6$) was quantified using the 'Image Lab' software and normalized by the protein content in each lane and then with respect to the average of control animals, thus setting the mean of control group as equal to a value of 1.

4.4.5 | Immunohistochemistry

Small tissue samples (~1.5 mm^2) were excised from fixed gill pouches and washed in 0.2% Triton-X 100 in PBS (PBST) on a motorized rotator (3 × 20 min), then blocked in PBST containing normal goat serum (1:50) and keyhole limpet hemocyanin (1:5000). Samples were incubated with mouse monoclonal α-NKA antibody (44 ng/ml) and rabbit polyclonal α-hagfish Rh antibodies (312.5 ng/ml) in blocking buffer overnight at room temperature. Samples were washed in PBST (3 × 15 min) both prior to and following 2 h of incubation with commercial ALEXA-fluor 2° antibodies (Invitrogen) (1:5000). Samples were imaged on a Zeiss Observer Z1 inverted microscope with LSM 800 confocal and super-resolution AiryScan detector (Carl Zeiss AG, Oberkochen, Germany). Micrographs and z-section stacks were cropped and adjusted for brightness and contrast using ZenBlue v2.6. z-stack images were re-rendered on Imaris (v 9.3.1, Oxford Instruments, Bitplane, Switzerland).

4.5 | Calculations and statistics

4.5.1 | Determination of ammonia speciation in blood and water

Blood/plasma and water pH and T_{amm} were utilized to calculate the speciation of ammonia based on the rearrangement of the Henderson-Hasselbach equation[54] as follows:

$$[NH_{4^+}] = \frac{[T_{amm}]}{1 + 10^{pH-pKa}} \quad (4)$$

$$[NH_3] = [T_{amm}] - [NH_{4^+}] \quad (5)$$

where pH and T_{amm} are the respective water or blood/plasma values, and pKa is the appropriate apparent dissociation constant for T_{amm} calculated from nomograms as a function of salinity, temperature, and blood/water pH.[55]

The partial pressure of NH_3 (P_{NH_3}) in plasma and water ($P_{NH_3}^{plasma}$ and $P_{NH_3}^{water}$, respectively) was calculated using the output from[2] above, along with the solubility coefficient for NH_3 (αNH_3) in seawater at 12°C as outlined in Boutilier et al.[56]:

$$P_{NH_3} = \frac{[NH_3]}{\alpha NH_3} \quad (6)$$

where P_{NH_3} is expressed in μtorr. The plasma to water NH_3 diffusion gradient ΔP_{NH_3} was thereafter calculated as:

$$\Delta P_{NH_3} = P_{NH_3}^{plasma} - P_{NH_3}^{Water} \quad (7)$$

whereby positive ΔP_{NH_3} values denote an outwardly directed partial pressure gradient for NH_3.

Plasma to water Nernst equilibrium potentials for NH_4^+ gradients ($E_{NH_4^+}$) was calculated using the appropriate gas constant (R), Faraday's constant, and the valence of NH_4^+ at the appropriate temperature in °K (12°C = 285°K) as follows:

$$E_{NH_4^+} = 56.1\ log\left(\frac{[NH_4^+]^{water}}{[NH_4^+]^{plasma}}\right) \quad (8)$$

where $[NH_4^+]^{water}$ and $[NH_4^+]^{plasma}$ are the respective [NH_4^+] in water and plasma and negative $E_{NH_4^+}$ values denote an outwardly directed NH_4^+ gradient.

4.5.2 | Quantification of ammonium flux (J_{NH4+}) using ^{14}C-MA radioactivity

Since hagfish pre-exposed to HEA had greater $[T_{amm}]_p$ than those pre-exposed to control conditions, it was necessary to account for the mismatch of relative ^{14}C-MA and NH_4^+ availability as it pertained to substrate availability and the calculation of isotopic specific activity. Thus, we calculated plasma [NH_4^+] loads in control and HEA exposed animals which were used with ^{14}C-MA measurements to estimate ammonium flux (J_{NH4+}) as:

$$J_{NH_4^+} = \left[\left(CPM_f^{water} - CPM_i^{water}\right) \bullet \frac{1}{m} \bullet \frac{1}{\Delta t}\right] \bullet \left[\frac{\frac{[NH_4^+]_i^{plasma} \bullet V_i^{plasma}}{CPM_i^{plasma}} + \frac{[NH_4^+]_f^{plasma} \bullet V_f^{plasma}}{CPM_f^{plasma}}}{2}\right] \quad (9)$$

where CPM^{water} denotes the CPMs in the final and initial water samples, m represents the animal mass (g), Δt refers to the delta time of the flux period, and $[NH_4^+]^{plasma}$, V^{plasma} and CPM^{plasma} denote the initial and final [NH_4^+] volume and CPMs in the plasma sample respectively.

In isolated gill pouch experiments, ^{14}C-MA flux from perfusate to perifusate was measured in the presence of DMSO (control) or amiloride (500 μM dissolved in DMSO) and $J_{NH_4^+}$ was calculated as:

$$J_{NH_4^+} = \left[\left(CPM_f^{peri} - CPM_i^{peri}\right) \bullet \frac{1}{m_t} \bullet \frac{1}{\Delta t}\right] \bullet \frac{[NH_4^+]^{perf} \bullet V^{perf}}{CPM^{perf}} \quad (10)$$

where CPM^{peri} denotes the CPMs in the final (collected sample) and initial (stock perifusate solution) perifusate samples, m_t represents the dry tissue mass of the gill pouch, Δt refers to the delta time of the flux period, and CPM^{perf}, V^{perf}, and $[NH_4^+]^{perf}$ denote the CPMs, volume, and [NH_4^+] in the perfusate sample, respectively. Calculated J_{NH4+} values for control and amiloride trials were averaged across 2 replicate trials on a single gill pouch preparation.

Given the known differences between ^{14}C-MA and ammonia structure and chemistry including different acid-dissociation constants which could influence estimates of actual ammonia excretion rate due to slight differences in the speciation of MA, analysis of these data were interpreted under assumptions that 1) NH_4^+ and MA^+ are transported by the same transporters,[21,59] 2) there is competition for transporter binding sites,[60] 3) if there are changes in affinity for MA^+ and NH_4^+, these will be similar for both molecules.

4.5.3 | Statistics

All statistical analyses were completed using GraphPad Prism 9.3.0 (GraphPad Software, San Diego, USA). Data are presented as means ± s.e.m. and were tested to meet the assumptions of normality and homoscedasticity. Measured values of $[T_{amm}]_w$ from Experiment 1 were analyzed by linear regression analysis. Two-way repeated measures ANOVA with the Geisser–Greenhouse correction was used to analyze differences in pH_w and pCO_2 data from Experiment 1 as well as $[T_{amm}]_p$ in Experiment 3. $[T_{amm}]_p$, ΔpNH_3 and E_{NH4}^+ data in Experiment 2 and J_{NH4+} data from Experiment 4 were analyzed using Ordinary two-way ANOVA. J_{NH4+} data from Experiment 5 were analyzed via one-tailed repeated measures Student's t-test with equal variances assumed. Differences amongst comparisons were determined via Dunnent's *or* Tukey's multiple comparisons post hoc analysis where appropriate. Statistical significance was assessed at $p < 0.05$.

ACKNOWLEDGMENTS

The authors wish to thank the three anonymous reviewers for their time and valuable feedback through the review process, BMSC Foreshore and Research staff, Drs. Chris Wood (UBC), Dave Randall (UBC), Samuel Starko (UBC) and Till Harter (SIO) for stimulating discussions, and finally Phil Zerofski, Anna Blanchard, and Ryan Myers for help with animal care. The data that support the findings of this study are available on Dryad at doi:10.6076/D1B01D

FUNDING INFORMATION

AMC was supported by a Scripps Institution Oceanography Postdoctoral Research Scholar Fellowship. GGG (Grant number 702306) and MPW (Grant number 04248) were funded by National Science Engineering Research Council (NSERC), MT (award no. 1754994) and SLE (award no. IOS-1121369) were funded by a National Science Foundation (NSF) grant.

CONFLICT OF INTEREST

The authors declare no competing interests.

ORCID

Alexander M. Clifford https://orcid.org/0000-0002-2836-5832
Michael P. Wilkie https://orcid.org/0000-0002-3844-8033
Martin Tresguerres https://orcid.org/0000-0002-7090-9266
Greg G. Goss https://orcid.org/0000-0003-0786-8868

REFERENCES

1. Smith CR, Baco AR. Ecology of whale falls at the deep-sea floor. *Oceanogr Mar Biol*. 2003;41:311-354.
2. Smith CR, Glover AG, Treude T, Higgs ND, Amon DJ. Whale-fall ecosystems: recent insights into ecology, paleoecology, and evolution. *Ann Rev Mar Sci*. 2015;7:571-596.
3. Martini F, Lesser M, Heiser JB. Ecology of the hagfish, *Myxine glutinosa* L., in the gulf of Maine: II. Potential impact on benthic communities and commercial fisheries. *J Exp Mar Biol Ecol*. 1997;214(1–2):97-106.
4. Clifford AM, Goss GG, Roa JN, Tresguerres M. Acid/base and ionic regulation in hagfish. In: Edwards SL, Goss GG, eds. *Hagfish Biology*. CRC Press; 2015:277-297.
5. Martini FH. The ecology of hagfishes. *The Biology of Hagfishes*. Springer Netherlands; 1998:57-77.
6. Baker DW, Sardella B, Rummer JL, Sackville M, Brauner CJ. Hagfish: champions of CO_2 tolerance question the origins of vertebrate gill function. *Sci Rep*. 2015;5:11182.
7. Clifford AM, Weinrauch AM, Goss GG. Dropping the base: recovery from extreme hypercarbia in the CO_2 tolerant Pacific hagfish (*Eptatretus stoutii*). *J Comp Physiol B*. 2018;188(3):421-435.
8. Braun MH, Perry SF. Ammonia and urea excretion in the Pacific hagfish *Eptatretus stoutii*: evidence for the involvement of rh and UT proteins. *Comp Biochem Physiol Part A Mol Integr Physiol*. 2010;157(4):405-415.
9. Clifford AM, Goss GG, Wilkie MP. Adaptations of a deep sea scavenger: high ammonia tolerance and active NH_4^+ excretion by the Pacific hagfish (*Eptatretus stoutii*). *Comp Biochem Physiol Part A Mol Integr Physiol.* 2015;182C:64-74.
10. Sidell BD, Stowe DB, Hansen CA. Carbohydrate is the preferred metabolic fuel of the hagfish (*Myxinie glutinosa*) heart. *Physiol Zool*. 1984;57:266-273.
11. Wells RM, Forster ME, Davison W, Taylor HH, Davie PS, Satchell GH. Blood oxygen transport in the free-swimming hagfish. *Eptatretus Cirrhatus J Exp Biol*. 1986;123:43-53.
12. Forster ME. Confirmation of the low metabolic rate of hagfish. *Comp Biochem Physiol Part A Mol Integr Physiol.* 1990;96(1):113-116.
13. Clifford AM, Zimmer AM, Wood CM, Goss GG. It's all in the gills: evaluation of O_2 uptake in Pacific hagfish refutes a major respiratory role for the skin. *J Exp Biol*. 2016;219(18):2814-2818.
14. Parks SK, Tresguerres M, Goss GG. Blood and gill responses to HCl infusions in the Pacific hagfish (*Eptatretus stoutii*). *Can J Zool*. 2007;85(8):855-862.
15. Clifford AM, Guffey SC, Goss GG. Extrabranchial mechanisms of systemic pH recovery in hagfish (*Eptatretus stoutii*). *Comp Biochem Physiol Part A Mol Integr Physiol.* 2014;168:82-89.
16. McDonald DG, Cavdek V, Calvert L, Milligan CL. Acid-base regulation in the Atlantic hagfish *Myxine glutinosa*. *J Exp Biol*. 1991;161:201-215.
17. Tresguerres M, Parks SK, Goss GG. Recovery from blood alkalosis in the Pacific hagfish (*Eptatretus stoutii*): involvement of gill V–H^+–ATPase and Na^+/K^+–ATPase. *Comp Biochem Physiol Part A Mol Integr Physiol.* 2007;148(1):133-141.
18. Evans DH, Piermarini PM, Choe KP. The multifunctional fish gill: dominant site of gas exchange, osmoregulation, acid-base regulation, and excretion of nitrogenous waste. *Physiol Rev*. 2005;85:97-177.
19. Heisler N. Acid-base regulation in fishes. In: Heisler N, ed. *Acid-Base Regulation in Animals*. Elsevier Biomedical Press; 1986:309-356.
20. Ip YK, Chew SF, Randall DJ. Ammonia toxicity, tolerance, and excretion. *Fish Physiology: Nitrogen Excretion*. Elsevier; 2001:109-148.
21. Nakada T, Westhoff CM, Kato A, Hirose S. Ammonia secretion from fish gill depends on a set of rh glycoproteins. *FASEB J*. 2007;21(4):1067-1074.
22. Wright PA, Wood CM. A new paradigm for ammonia excretion in aquatic animals: role of rhesus (rh) glycoproteins. *J Exp Biol*. 2009;212(Pt 15):2303-2312.
23. Edwards SL, Arnold J, Blair SD, et al. Ammonia excretion in the Atlantic hagfish (*Myxine glutinosa*) and responses of an Rhc glycoprotein. *Am J Physiol Regul Integr Comp Physiol*. 2015;308(9):R769-R778.
24. Weiner ID, Verlander JW. Ammonia transporters and their role in acid-base balance. *Physiol Rev*. 2017;97(2):465-494.
25. Tresguerres M, Clifford AM, Harter TS, et al. Evolutionary links between intra- and extracellular acid–base regulation in fish and other aquatic animals. *J Exp Zool A Ecol Integr Physiol*. 2020;333(6):449-465.
26. Clifford AM, Weinrauch AM, Edwards SL, Wilkie MP, Goss GG. Flexible ammonia handling strategies using both cutaneous and branchial epithelia in the highly ammonia tolerant Pacific hagfish. *Am J Physiol Regul Integr Comp Physiol*. 2017;313(2):R78-R90.
27. Saha N, Ratha BK. Functional ureogenesis and adaptation to ammonia metabolism in Indian freshwater air-breathing catfishes. *Fish Physiol Biochem*. 2007;33(4):283-295.
28. Chew SF, Jin Y, Ip YK. The loach *Misgurnus anguillicaudatus* reduces amino acid catabolism and accumulates alanine and glutamine during aerial exposure. *Physiol Biochem Zool*. 2001;74:226-237.
29. Eom J, Giacomin M, Clifford AM, Goss GG, Wood CM. Ventilatory sensitivity to ammonia in the Pacific hagfish (*Eptatretus stoutii*), a representative of the oldest extant connection to the ancestral vertebrates. *J Exp Biol*. 2019;222(14):jeb.199794.

30. Krogh A. The active absorption of ions in some freshwater animals. *Z f Vergl Physiologie*. 1938;25(3):335-350.
31. Blanchard A, Eladari D, Leviel F, Tsimaratos M, Paillard M, Podevin R-A. NH_4^+ as a substrate for apical and basolateral Na^+-H^+ exchangers of thick ascending limbs of rat kidney: evidence from isolated membranes. *J Physiol*. 1998;506(Pt 3):689-698.
32. Wöhlert D, Kühlbrandt W, Yildiz Ö. Structure and substrate ion binding in the sodium/proton antiporter PaNhaP. *Elife*. 2014;3:e03579.
33. Randall DJ, Wilson JM, Peng KW, et al. The mudskipper, *Periophthalmodon schlosseri*, actively transports NH_4^+ against a concentration gradient. *Am J Physiol Regul Integr Comp Physiol*. 1999;277(6 Pt 2):R1562-R1567.
34. Tresguerres M, Parks SK, Goss GG. V-H^+-ATPase, Na^+/K^+-ATPase and NHE2 immunoreactivity in the gill epithelium of the Pacific hagfish (*Eptatretus stoutii*). *Comp Biochem Physiol Part A Mol Integr Physiol.* 2006;145(3):312-321.
35. Edwards SL, Claiborne JB, Morrison-Shetlar AI, Toop T. Expression of Na^+/H^+ exchanger mRNA in the gills of the Atlantic hagfish (*Myxine glutinosa*) in response to metabolic acidosis. *Comp Biochem Physiol Part A Mol Integr Physiol.* 2001;130(1):81-91.
36. Carter DO, Yellowlees D, Tibbett M. Cadaver decomposition in terrestrial ecosystems. *Naturwissenschaften*. 2007;94(1):12-24.
37. Wilkie MP, Wang Y, Walsh PJ, Youson JH. Nitrogenous waste excretion by the larvae of a phylogenetically ancient vertebrate: the sea lamprey (*Petromyzon marinus*). *Can J Zool*. 1999;77(5):707-715.
38. Boussiba S, Gibson J. Ammonia translocation in cyanobacteria. *FEMS Microbiol Lett*. 1991;88(1):1-14.
39. Bishop JM, Verlander JW, Lee H-W, et al. Role of the rhesus glycoprotein, rh B glycoprotein, in renal ammonia excretion. *Am J Physiol Renal Physiol*. 2010;299(5):F1065-F1077.
40. Weihrauch D, Ziegler A, Siebers D, Towle DW. Active ammonia excretion across the gills of the green shore crab *Carcinus maenas*: participation of Na^+/K^+-ATPase, V-type H^+-ATPase and functional microtubules. *J Exp Biol*. 2002;205:2765-2775.
41. Nawata CM, Hung CCY, Tsui TKN, Wilson JM, Wright PA, Wood CM. Ammonia excretion in rainbow trout (*Oncorhynchus mykiss*): evidence for rh glycoprotein and H^+-ATPase involvement. *Physiol Genomics*. 2007;31(3):463-474.
42. Kleyman TR, Cragoe EJ. Amiloride and its analogs as tools in the study of ion transport. *J Membr Biol*. 1988;105(1):1-21.
43. Blair S, Li X, Dutta D, Chamot D, Fliegel L, Goss G. Rainbow trout (Oncorhynchus mykiss) Na^+/H^+ exchangers tNhe3a and tNhe3b display unique inhibitory profiles dissimilar from mammalian NHE isoforms. *Int J Mol Sci*. 2021;22(4):2205.
44. Avella M, Bornancin M. A new analysis of ammonia and sodium transport through the gills of the freshwater rainbow trout (*Salmo gairdneri*). *J Exp Biol*. 1989;142:155-117.
45. Parks SK, Tresguerres M, Goss GG. Theoretical considerations underlying Na^+ uptake mechanisms in freshwater fishes. *Comp Biochem Physiol Part C Toxicol Pharmacol*. 2008;148(4):411-418.
46. Clifford AM, Tresguerres M, Goss GG, Wood CM. A novel K^+-dependent Na^+ uptake mechanism during low pH exposure in adult zebrafish (*Danio rerio*): new tricks for old dogma. *Acta Physiol*. 2022;234(3):e13777.
47. Goss GG, Wood CM. Two-substrate kinetic analysis: a novel approach linking ion and acid-base transport at the gills of freshwater trout. *Oncorhynchus Mykiss J Comp Physiol B*. 1991;161(6):635-646.
48. Good DW, Knepper MA. Ammonia transport in the mammalian kidney. *Am J Physiol Renal Physiol*. 1985;248(4):F459-F471.
49. Mudry B, Guy RH, Delgado-Charro MB. Transport numbers in transdermal iontophoresis. *Biophys J*. 2006;90(8):2822-2830.
50. Bardack D. First fossil hagfish (Myxinoidea): a record from the Pennsylvanian of Illinois. *Science (New York, NY)*. 1991;254(5032):701-703.
51. Forster ME, Fenwick JC. Stimulation of calcium efflux from the hagfish, *Eptatretus cirrhatus*, gill pouch by an extract of corpuscles of Stannius from an eel (*Anguilla dieffenbachii*): Teleostei. *Gen Comp Endocrinol*. 1994;94(1):92-103.
52. Dymowska AK, Schultz AG, Blair SD, Chamot D, Goss GG. Acid-sensing ion channels are involved in epithelial Na^+ uptake in the rainbow trout *Oncorhynchus mykiss*. *Am J Physiol Cell Physiol*. 2014;307(3):C255-C265.
53. Verdouw H, Van Echteld C, Dekkers E. Ammonia determination based on indophenol formation with sodium salicylate. *Water Res*. 1978;12:399-402.
54. Wright PA, Wood CM. An analysis of branchial ammonia excretion in the freshwater rainbow trout: effects of environmental pH change and sodium uptake blockade. *J Exp Biol*. 1985;114(1):329-353.
55. Cameron JN, Heisler N. Studies of ammonia in the Rainbow trout: physico-chemical parameters, acid-base behaviour and respiratory clearance. *J Exp Biol*. 1983;105:107-125.
56. Boutilier RG, Heming TA, Iwama GK. Physicochemical parameters for use in fish respiratory physiology. In: Hoar WS, Randall DJ, eds. *Fish Physiology*. New York; 1984:403-426.
57. Lebovitz RM, Takeyasu K, Fambrough DM. Molecular characterization and expression of the (Na^+ + K^+)-ATPase alpha-subunit in *Drosophila melanogaster*. *EMBO J*. 1989;8(1):193-202.
58. Kwan GT, Tresguerres M. Elucidating the acid-base mechanisms underlying otolith overgrowth in fish exposed to ocean acidification. *Sci Total Environ*. 2022;823:153690.
59. Nakhoul NL, Hamm LL. Non-erythroid rh glycoproteins: a putative new family of mammalian ammonium transporters. *Pflugers Arch Eur J Physiol*. 2004;447(5):807-812.
60. Westhoff CM, Ferreri-Jacobia M, Mak D-OD, Foskett JK. Identification of the erythrocyte rh blood group glycoprotein as a mammalian ammonium transporter. *J Biol Chem*. 2002;277(15):12499-12502.

SUPPORTING INFORMATION

Additional supporting information may be found in the online version of the article at the publisher's website.

How to cite this article: Clifford AM, Wilkie MP, Edwards SL, Tresguerres M, Goss GG. Dining on the dead in the deep: Active NH_4^+ excretion via $Na^+/H^+(NH_4^+)$ exchange in the highly ammonia tolerant Pacific hagfish, *Eptatretus stoutii*. *Acta Physiol*. 2022;00:e13845. doi: 10.1111/apha.13845

Electronic Supplementary Information

For Research Article:

Dining on the dead in the deep sea: a mechanism for active NH_4^+ excretion in gills from the highly ammonia tolerant Pacific hagfish (*Eptatretus Stoutii*)

Alexander M. Clifford*[1,2,3], Michael P. Wilkie[4], Susan L. Edwards[5], Martin Tresguerres[#1], Greg G. Goss[#2,3]

1. Marine Biology Research Division, Scripps Institution of Oceanography, University of California, 9500 Gilman Drive, San Diego, La Jolla, CA 92093-0202.
2. Department of Biological Sciences, University of Alberta, 116 St. and 85 Ave., Edmonton, Alberta, T6G 2R3, Canada
3. Bamfield Marine Sciences Centre, 100 Pachena Rd., Bamfield, British Columbia, V0R 1B0, Canada
4. Department of Biology and Laurier Institute for Water Science, Wilfrid Laurier University, Waterloo, Ontario, N2L 3C5
5. Department of Biological Sciences, Wright State University, Dayton, Ohio, 45435-0001, USA

*corresponding author: aclifford@ucsd.edu

[#]equal contributors

Contents:

Supplementary Figures

Supplementary Movies

Supplementary Figure Legends

SI Figure 1: *Western blots* (*a)*lanes of a 10% SDS-Page gel were loaded with 10 µg protein from gills from either Control or 24 h 10 mM HEA exposed hagfish. Primary incubations were with 1:2000 of polyclonal rabbit anti-Atlantic hagfish antibody (band size ~50 kDa). Longer exposures or higher protein loading did not reveal any additional bands. (*b*) Ponceau S staining of Western blot membranes. Following imaging, membranes were soaked in a 0.1% (w/v) solution of Ponceau S to stain total protein to confirm equal loading across lanes.

SI Video 1: *Movie of dually perfused/perifused hagfish gill*. A single hagfish gill pouch was isolated and prepared (*see methods*), and then perfused with blue food coloring within the vascular compartment.

SI Figure 1

